ELECTRODIAGNOSTICS OF DISEASES WITH CONCENTRIC VISUAL FIELD DEFECTS

Ph. D. Thesis

Andrea Pálffy M.D.

Department of Ophthalmology

Faculty of Medicine

University of Szeged

Szeged, Hungary

2010

Publications related to the thesis:

I. Janáky M**, Pálffy A,** Kolozsvári L, Benedek Gy: Unilateral manifestation of melanoma-associated retinopathy. *Archives of Ophthalmology* 2002; 120: 866-67.

II. Janáky M, Fülöp Zs, **Pálffy A**, Benedek K, Benedek Gy.: Non-arteritic ischaemic optic neuropathy (NAION) in patients under 50 years of age. *Acta Ophthalmologica Scandinavica* 2005; 83: 499-503.

III. Janáky M, Fülöp Zs, **Pálffy A**, Benedek K, Benedek Gy: Electrophysiological findings in patients with nonarteritic anterior ischemic optic neuropathy. *Clinical Neurophysiology* 2006; 117: 1158-66.

IV. **Pálffy A**, Szilágyi M, Benedek K: Differential diagnosis of concentric visual field defects using electrophysiological methods. *Szemészet* 2006; 143: 64-68.

V. Janáky M, **Pálffy A**, Fülöp ZS, Szabó Á, Gyetvai T, Liszli P: Differential diagnostics of nonarteritic anterior ischaemic optic neuropathy (NAION). *Szemészet* 2006; 143: 17-21.

VI. Janáky M, **Pálffy A**, Deák A, Szilágyi M, Benedek Gy: Multifocal ERG reveals several patterns of cone degeneration in retinitis pigmentosa with concentric narrowing of the visual field. *Investigative Ophthalmology and Visual Science* 2007; 48: 383-89.

VII. Janáky M, **Pálffy A**, Horváth Gy, Tuboly G, Benedek Gy: Pattern-reversal electroretinograms and visual evoked potentials in retinitis pigmentosa. *Documenta Ophthalmologica.* Advances in ophthalmology 2008; 117: 27-36.

VIII. **Pálffy A**, Janáky M, Fejes I, Horváth G, Benedek G: Interocular amplitude differences of multifocal electroretinograms obtained under monocular and binocular stimulation conditions. *Acta Physiologica* (Accepted to publication)

Publications not related to the thesis:

IX. Janáky M, **Pálffy A**, Deák A, Gallyas É, Benedek Gy: Electrophysiological screening of hereditary diseases in myopic patients. *Szemészet* 2002; 139: 217-221.

X. **Pálffy A**, Gyetvai T, Janáky M, Kolozsvári L: Bilateral metastases of breast cancer – case report *Szemészet* 2003; 140: 259-62.

XI. Janáky M, **Pálffy A**, Fülöp Zs, Szabó Á, Gyetvai T, Liszli P: Paraneoplastic syndromes of the retina. Description of a case of melanoma-associated retinopathy. *Szemészet* 2003; 140: 37-41.

XII. Janáky M, **Pálffy A,** Benedek K, Benedek Gy.: New chapter in the study of visual evoked potentials - clinical application of the multifocal VEP method. *Ideggyógyászati Szemle* 2004; 57: 377-83.

XIII. Janáky M, **Pálffy A**, Benedek K, Benedek Gy: New chapter in visual evoked potential studies: Clinical application of the multifocal VEP method. *Ideggyógyászati Szemle* 2004; 57: 377–83.

XIV. Gyetvai T, **Pálffy A**, Vízvári E: Postoperative endophthalmitis: a 6 year-review. *Szemészet* 2006; 143: 43-45.

XV. Benedek K, **Pálffy A**, Bencsik K, Fejes I, Rajda C, Tuboly G, Liszli P: Combined use of pattern electroretinography and pattern visual evoked potentials in neuroophthalmological practice. *Ideggyógyászati Szemle* 2008; 61: 33-41.

Abbreviations

AD autosomal dominant
AION arteritic ischaemic optic neuropathy
ANOVA analysis of variance
AR autosomal recessive
CAR carcinoma-associated retinopathy
CSF cerebrospinal fluid
CV coefficients of variability
DNA deoxyribonucleic acid
DTL Dawson-Trick-Litzkow
ERG electroretinography
FVEP flash visual evoked potential
GABA gamma-aminobutyric acid
IOP intraocular pressure
ISCEV International Society of Clinical Electrophysiology of Vision
MAR melanoma associated retinopathy
mfERG multifocal electroretinography
mfVEP multifocal visual evoked potential
MRI Magnetic Resonance Imaging
NAION nonarteritic anterior ischemic neuropathy
OP oscillatory potential
PERG pattern electroretinography
PVEP pattern visual evoked potential
RCT retino-cortical time
RP retinitis pigmentosa
RPE retinal pigmentepithel
S simplex
SD standard deviation
U Usher syndrome
VA visual acuity
VEP visual evoked potential
VF visual field
XL-R x-linked recessive

Contents

1. Introduction

Interpretation of the visual field (VF) is a key part of ophthalmic and neurological examinations. A VF defect indicates a defect in the retina or in the visual pathways. The damage may affect different locations along the visual pathway, from the optic nerve to the visual centres of the occipital lobes. Beyond characterizing almost all pathological processes in the region, VF defects also help to locate the site of the lesion, as lesions interrupting the function of particular parts of the visual pathway cause specific defects. Thus, perimetric examination may indicate the site and extent of damage to the visual pathway.

The extent of the involvement of the visual pathway may change during the progression of the pathological process. In cases with concentric VF narrowing and generalised sensitivity disturbances the VF defect can be described according to alterations by retinal quadrants. The depression may be equal or unequal by meridians.

Progression may lead to tunnel vision, by which means a field narrowing yielding 20º or less residual area on one or both sides is meant. Depending on in which quadrant the larger isopter constriction is found and in which stage of the disease the characteristic field defect turns into no longer specific VF constriction, a problem of differential diagnostics also arises.

Retinitis pigmentosa (RP) is a disease with a characteristic tubular field defect, although it occurs only at the end stage of the disease. The appearance of tunnel vision is not a pathognomonic sign of RP, since it can develop in other ophthalmological, optic nerve and intracranial diseases, e.g. in toxic and ischaemic optic neuropathies, paraneoplastic syndromes, and retrobulbar processes (like intraorbital infiltration of tumors, endocrine orbitopathy, etc.) as well. It occurs also in neurological, neuroophthalmological diseases, for example in diseases with generalized intracranial pressure elevation, direct compression of the visual pathway, or inflammatory processes and vascular disturbances.

Non-organic causes of VF defects occur in psychiatric diseases (e.g. hysteric amblyopia), or in case of malingering (visually handicapped benefits, court cases).

For objective detection of the functional alterations in the visual pathway numerous electrophysiological methods have been developed in the past two decades. These include the standard electroretinography (ERG), multifocal electroretinography (mfERG), pattern electroretinography (PERG), visual evoked potential (VEP) and the multifocal visual evoked potential (mfVEP). The importance of these methods is that the retinal function can be tested in detail, and minimal cooperation of the patient is sufficient to obtain objective data on the function of the retina, the visual pathway and the visual cortex.

The aim of our study was to assess the value of the electrophysiological methods in the differential diagnosis and in the localisation of the defect in diseases with VF alterations. We

sought to determine which electrophysiological method(s) can help the detection of the cause of non-characteristic VF defects, and which combination of methods yields the best localisation of the lesion.

2. General description of methods

2.1. Techniques of visual field testing

There are many methods to evaluate the function of the visual pathways (confrontation testing, Amsler test, kinetic and static perimetry). The most widely used ones are the kinetic perimetry (Goldmann perimetry) and the automatic, static method (Humphrey-test, Octopus perimetry). The selection of the appropriate technique is based on the patient's history, on the clinical symptoms (central or peripheral visual disturbances), on the VA, on the ophthalmoscopic findings (protrusion of the disc: papilloedema, paled optic nerve head or excavation of the optic nerve head) and on the aetiology of the particular disease. VF examinations, regardless of which method is used, should never be interpreted without considering other clinical data, such as the patient's age, mental and ophthalmological status. One also has to keep in mind that all of these tests are subjective.

In kinetic perimetry, spots of equal retinal sensitivity in the VF are searched for. By connecting these areas of equal sensitivity, an isopter is defined. A stimulus of constant size and intensity is used, which is moved from blind to detectable areas of the VF along a meridian. The luminance and the size of the target can be changed to plot different isopters. The larger the size and higher the intensity of the target, the wider the isopter is. This method is the one most widely used in detecting VF narrowing. The method is both patient-friendly and time-effective.

In static perimetry we use stationary targets of constant size, but variable intensity. With this type of perimetry we measure differential light sensitivity for a stimulus presented against a constant background illumination. The threshold of this differential light sensitivity represents the brightness of the stimulus that is actually perceived. Thus, this method indicates retinal light sensitivity at predetermined locations in the VF.

2.2. Electrophysiological methods

2.2.1. Electroretinography (ERG)

Full-field electroretinography is a well-established non-invasive technique that reveals the electrical activity generated within the retina in response to light stimulation. Different conditions of retinal adaptation and stimulus intensity make the assessment of global function of rod and cone pathways and the functional segregation of different retinal layers possible.

The ERG components are influenced by numerous external and internal factors, such as dark adaptation of the retina, stimulus intensity, stimulus wavelength, frequency of stimulation, stimulus duration, size of illuminated retinal area, clarity of media, retinal development, pupil size, age, sex, refractive errors, circulation of blood, drugs, anaesthesia, and so on.

Considering these factors, the International Society of Clinical Electrophysiology of Vision (ISCEV) has determined the standard clinical protocols to facilitate inter-laboratory comparison. An ISCEV standard ERG includes the following responses, named according to retinal adaptation level and the intensity of the stimulus (flash strength in $cd \cdot s \cdot m^{-2}$): (1) Dark-adapted 0.01 ERG (formerly 'rod response') consisting of a negative 'a' wave representing the rod function and a positive 'b' wave generated mainly by the bipolar cells.[] (2) Dark-adapted 3.0 ERG (formerly 'maximal or standard combined rod–cone response'). It is a mixed rod-cone response dominated by rod system function. The negative 'a' wave arises in relation to photoreceptor hyperpolarisation.[] The large 'b' wave reflects postphototransduction or postreceptoral function.[] (3) Dark-adapted 3.0 oscillatory potentials (OP) (formerly 'oscillatory potentials') consist of small wavelets from the ascending limb of the 'b' wave of maximal ERG, and they are at least partially generated by the amacrine cells. (4) Light-adapted 3.0 ERG (formerly 'single-flash cone response') reflects activity of the cone system. Its 'a' wave is generated by the cone receptors and the 'b' wave comes from the hyperpolarizing ON and OFF bipolar cells. (5) Light-adapted 3.0 flicker ERG (formerly '30 Hz flicker') arises from the L and M cone pathways, because the S cone system is relatively insensitive to high temporal frequencies.

2.2.2. Multifocal electroretinography (mfERG)

Multifocal electroretinography (mfERG) provides topographic measure of the electrophysiological activity of the central retina. Using this technique, multiple local cone-driven responses are recorded from the retina under light-adapted conditions.

The pattern of the stimulus contains an array of hexagons (61 or 103), that increase in size with distance from the centre. The sizes of the hexagons are scaled inversely to the gradient of cone receptor density, so as to produce focal responses of approximately equal amplitude in control subjects. The radius of the central hexagon is 2°. The retinal size of the display subtends 30º in radius, similar to the area tested by standard clinical VFs with automated perimetry. During stimulation, each element is either black or white. The stimulus contrast is 93%. During stimulation, the display appears to flicker because each hexagon goes through a pseudo-random sequence (the m-sequence) of black and white presentations. Each hexagon has a 50% chance of being white or black upon each frame change. Every hexagon in the array is driven by the same m-sequence of white and black presentations.

The typical waveform of the basic mfERG response (also called the first-order response or first-order kernel) is a biphasic wave with an initial negative deflection followed by a positive peak. There is usually a second negative deflection after the positive peak. These three peaks are called N1, P1 and N2, respectively.

There is evidence that N1 includes contributions from the same cells that contribute to the a-wave of the full-field cone ERG, and that P1 includes contributions from the cells contributing to the cone b-wave and OPs. Although there is some homology between the mfERG waveform and the conventional ERG, the stimulation rates are higher for the mfERG, and mfERG responses are mathematical abstractions. Thus, mfERG responses are not technically 'little ERG responses'.

2.2.3. Pattern electroretinography (PERG)

Pattern electroretinogram (PERG) is a retinal response evoked by viewing a temporally alternating black and white checkerboard pattern.

The waveform of the PERG depends on the temporal frequency of the stimulus. At high temporal frequencies, i.e. above 10 reversals/s (5 Hz), the successive waveforms overlap and a 'steady-state' PERG is evoked. The steady-state PERG waveform is roughly sinusoidal, and interpretation requires measurement of amplitude and phase shift by Fourier analysis.

At low temporal frequencies (<6 reversals per second (rev/s); equivalent to <3 Hz) transient PERGs are obtained, which are effectively complete before the next contrast reversal, thus allowing separation and interpretation of the components; this is the standard method for clinical practice.

The PERG waveform consists of a small initial negative component (N35), which is followed by a much larger positive component (P50). This, then, is followed by a larger negative component (N95).

The exact origins of P50 are yet to be ascertained, but it appears partially to arise in relation to spiking cell function, and partially from non-spiking cells. P50 is driven by the macular photoreceptors and has been used to provide an effective assessment of macular function. There is clinical and experimental evidence to indicate that N95 arises in the retinal ganglion cells.

2.2.4. Pattern visual evoked potential (PVEP)

VEP is an evoked electrophysiological potential extracted from the electroencephalographic activity of the occipital cortex and can be recorded at the scalp. It

provides important diagnostic information regarding the functional integrity of the visual system.[7]

VEPs can be evoked by flash (flash VEP, FVEP) or pattern stimulation (pattern VEP, PVEP). FVEP is not sensitive to VA loss, and its intraindividual variability is high. The flashing light stimulates both the parvocellular and the magnocellular pathways. Conduction velocities of these two pathways are different; thus, the responses may have two peaks. This method is applied only when the patient VA is not enough to fixate on the pattern stimulus, or patient cooperation is impaired.

In the clinical practice, a black and white checkerboard pattern is used for evoking PVEP. Field size, pattern size and contrast, retinal area of stimulation, and the rate of pattern presentation can all be varied.

PVEPs are either transient or steady-state. A transient PVEP is to be observed when a substantial interval elapses between stimulus presentations, allowing the brain to regain its resting state. Steady-state PVEPs are produced when the brain does not regain its resting state between stimulus presentations. The temporal rate at which PVEPs change from transient to steady-state varies, depending on a variety of factors, but in general the transition occurs at 6-10 presentation per second.

PVEP reflects activity of the sensory visual pathways from the central part of the retina to the occipital cortex. The projection of the macula is situated on the mesial surface of the occipital cortex. The other reason why PVEP reflects the activity of central retina is cortical magnification.[7] The magnification factor is 5.6 mm/degree at the fovea.

The fovea and the parafovea may be selectively stimulated changing the size of the squares. 10-15 min sized squares stimulate the fovea, while the larger, 50 min squares stimulate the parafovea.

3. Methods and results

3.1. Techniques of visual field testing

Kinetic VF tests were carried out with a Goldmann perimeter, with a background intensity of 3.15 apostilbs (asb). A III.e white target was moved from blind to detectable areas of the VF along a set meridian. The procedure was repeated with the use of the same stimulus along other meridians, usually spaced every 15°.

Static perimetry was carried out with an OCTOPUS perimeter 1-2-3 (Interzeag AG, Schlieren, Switzerland). The differential light sensitivity to a stimulus against a constant background illumination was measured.

3.2. Electrophysiological methods

Electroretinograms (ERGs), multifocal electroretinograms (mfERGs), pattern electroretinograms (PERGs) and visual evoked potentials (VEPs) were recorded with the RETI-Port 32 system (Roland Consult Gmbh, Wiesbaden, Germany). All of the procedures were performed in accordance with ISCEV standards.

Before the tests, the procedures were fully explained to the patients and their informed consent was obtained. The research followed the tenets of the Declaration of Helsinki.

In introducing these new methods into the routine clinical practice we determined first the parameters of the normal values and their variability.

Normal volunteers were free from ophthalmological and systemic diseases. Their VA was 1.0 on both eyes and the error of refraction was under +1.0 and -3.0 D. Before the tests, the appropriate refraction was determined and the vision was corrected for the testing distance.

Data were analyzed with SPSS 13 software (SPSS Inc., Chicago, USA). The normal data are presented mean, median, standard deviation (SD), percentiles 0.5 and 0.95, and coefficients of variability (CV).

Our data served as bases of evaluation of the retinal function. The results are comparable to the national and international results. The variability of our data is not larger than those of other laboratories.

3.2.1. Electroretinography (ERG)

Standard ERGs were studied in 31 volunteers with good vision. Mean age of the subjects was 37.2 ± 16.7 years (9-77 years).

The pupils of the volunteers were fully dilated with a combination of Mydrum (Chevin, Ankefarm) and Neosynephrin (10%, Ursaform) solutions before ERG testing.

Dawson-Trick-Litzkow (DTL) electrodes were routinely used as active electrodes. Gold cup electrodes, 5 mm in diameter, were used as reference electrodes applied 1 cm laterally from the ipsilateral orbital rim, and as a ground electrode, placed over the midline of the forehead (Fz). Sampling rate was 1000 Hz. Impedance was kept below 5 kΩ. Binocular stimulation was used.

ERGs were recorded by Ganzfeld (full-field) stimulator of RETI-Port 32. (1) Dark-adapted 0.01 ERG (rod response) was measured after a 20 minutes' dark adaptation. The stimulus was a dim white flash of 0.01 $cd \cdot s \cdot m^{-2}$; with a minimum interval of 2 s between flashes. (2) Dark-adapted 3.0 ERG (maximal response) was elicited by a white 3.0 $cd \cdot s \cdot m^{-2}$ flash in the dark-adapted eye. There was an interval of at least 10 s between stimuli. (3)

Dark-adapted OPs were obtained from the dark-adapted eye, using the 3.0 $cd \cdot s \cdot m^{-2}$ flash stimulus. (4) The eye was then restored to photopic conditions (rod-suppressing background illumination of 17-34 cd/m^2) and photopic responses were recorded. Light-adapted 3.0 ERG (single-flash cone response) was evoked by a 3.0 $cd \cdot s \cdot m^{-2}$ stimulus, with at least 0.5 s between flashes. (5) Light-adapted 3.0 flicker ERG (30 Hz flicker) was obtained with 3.0 $cd \cdot s \cdot m^{-2}$ stimuli. Flashes were presented at a rate of approximately 30 stimuli per second (30 Hz).

The representative ERG curves are presented in Figure 1.

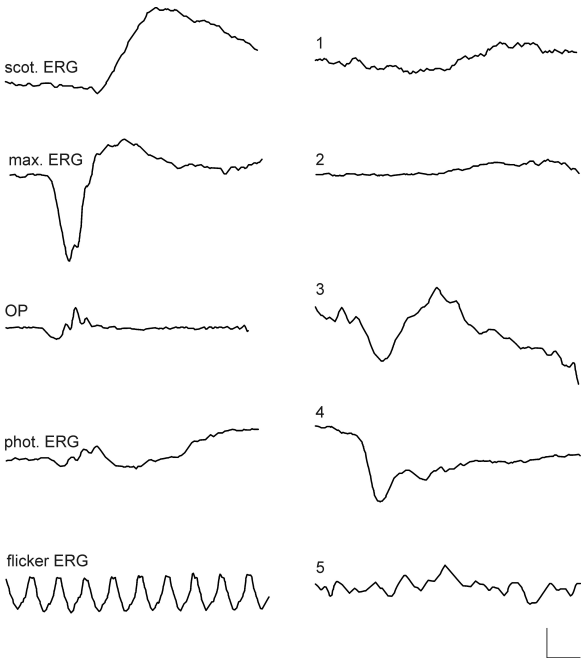

Figure 1. Electroretinograms of normal patients. ERGs are presented as continuous lines. Abscissa: time in ms, ordinate: amplitude in μV. Calibration: 6.2 μV, 25 ms.

The amplitudes and latencies were measured for the interpretation of the ERGs. The a-wave amplitude was measured from baseline to a-wave trough; the b-wave amplitude was measured from a-wave trough to b-wave peak; the a-wave and b-wave latencies were measured from the time of the flash to the peak of the wave.

The normal parameters of the waves are presented in Table 1.

Rod response	Mean	Median	SD	Percentile 05	Percentile 95	CV
a latency (ms)	35,13	38,00	6,15	21,25	42,35	0,18
b latency (ms)	77,38	79,00	8,32	58,40	88,70	0,11
a amplitude (μV)	22,93	14,30	36,06	1,71	101,97	1,57
b amplitude (μV)	250,44	238,50	76,07	155,30	399,65	0,30
Maximal response						
a latency (ms)	20,06	18,00	4,51	17,00	35,25	0,22
b latency (ms)	49,24	49,00	8,77	37,00	73,00	0,18
a amplitude (μV)	210,96	217,50	74,54	17,28	327,25	0,35
b amplitude (μV)	359,79	356,00	90,18	199,25	512,00	0,25
Oscillatory potential						
N1 latency (ms)	15,08	15,00	1,47	12,35	18,30	0,10
P1 latency (ms)	19,94	20,00	1,30	18,00	22,30	0,07
N2 latency (ms)	22,38	22,00	1,04	21,00	25,00	0,05
P2 latency (ms)	25,74	26,00	1,62	23,50	29,00	0,06
N3 latency (ms)	30,76	30,00	1,23	29,00	34,00	0,04
P3 latency (ms)	33,74	34,00	1,90	31,00	37,00	0,06
N4 latency (ms)	40,56	40,00	2,18	36,65	44,00	0,05
P4 latency (ms)	44,59	45,00	3,55	36,75	51,00	0,08
OS1 amplitude (μV)	44,63	44,80	14,64	21,23	72,25	0,33
OS2 amplitude (μV)	80,85	84,70	29,99	30,38	136,75	0,37
OS3 amplitude (μV)	19,41	16,70	12,27	2,77	43,25	0,63
OS4 amplitude (μV)	9,27	7,81	6,10	2,28	23,14	0,66
Single-flash cone response						
a latency (ms)	16,41	16,00	3,26	12,00	22,75	0,20
b latency (ms)	35,32	35,50	2,36	30,75	40,25	0,07
a amplitude (μV)	33,92	32,40	11,69	15,60	56,75	0,34
b amplitude (μV)	92,65	87,70	33,07	42,55	151,50	0,36
Flicker 30 Hz ERG						
N1 latency (ms)	15,24	14,00	3,51	11,40	23,40	0,23
P1 latency (ms)	29,79	30,00	1,65	27,00	32,30	0,06
flicker N1-P1 latency (ms)	86,53	80,90	28,54	35,16	151,60	0,33
30 Hz amplitude (μV)	33,55	32,00	10,99	20,70	56,70	0,33

Table 1. Normative ERG data in the group of healthy subjects with good vision. (SD: standard deviation, CV: coefficients of variability)

3.2.2. Multifocal electroretinography (mfERG)

21 volunteers with good vision were involved in this examination. Their ages ranged from 9 to 72 year with a mean of 33.24 ± 14.9 years. We also analyzed mfERG results obtained in 35 healthy volunteers with good vision. These provided no evidence for the advantage of either binocular or monocular stimulating conditions in obtaining mfERGs.

Volunteers' pupils were fully dilated with a combination of Mydrum (Chevin, Ankefarm) and Neosynephrin (10%, Ursaform) solutions before testing.

DTL electrodes were used as active recording electrodes. Gold cup electrodes, 5 mm in diameter, were used as reference electrodes applied 1 cm laterally from the ipsilateral orbital

rim and as ground electrode placed over the midline of the forehead (Fz). Sampling rate was 1000 Hz. Impedance was kept below 5 kΩ.

The screen–patient distance was 28 cm. Subjects had normal or corrected-to-normal VA (1.0). Binocular stimulation was used, but when we found the area of best responsiveness in an eccentric position, we retested the patient with monocular stimulation and compared the two recordings.

The subject fixated a small central sign in the display containing 61 hexagons. The radius of the central hexagon was 2°. The retinal size of the display subtended 30º, similar to the area tested by standard clinical VFs with automated perimetry.

During stimulation, each element was either black or white (93% contrast). The mean luminance was 51.8 cd/m^2, whereas the frame rate was 75 Hz. For a 50.000 times' amplification, the filters were set between 5 and 100 Hz. Typically the recording took about 7 min.

The mfERG responses had three peaks, N1, P1 and N2, respectively. The N1 response amplitude was measured from the starting baseline to the base of the N1 trough; the P1 response amplitude was measured from the N1 trough to the P1 peak. The peak times (implicit times) of N1 and P1 were measured from the stimulus onset.

Figure 2 shows a single mfERG response.

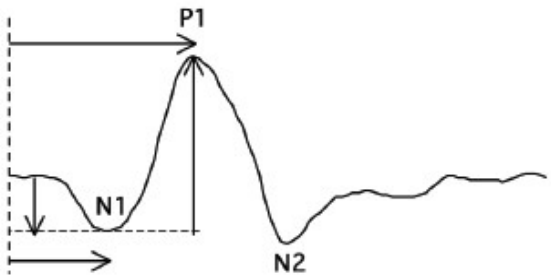

Figure 2. A schematic single mfERG response to illustrate the major features of the waveform.

The results were displayed as trace arrays, group averages, quadrants and topographic (3D) response density plots (Figure 3). Trace arrays can produce an array of the mfERG traces. This display of the results is useful for visualizing areas of abnormality.

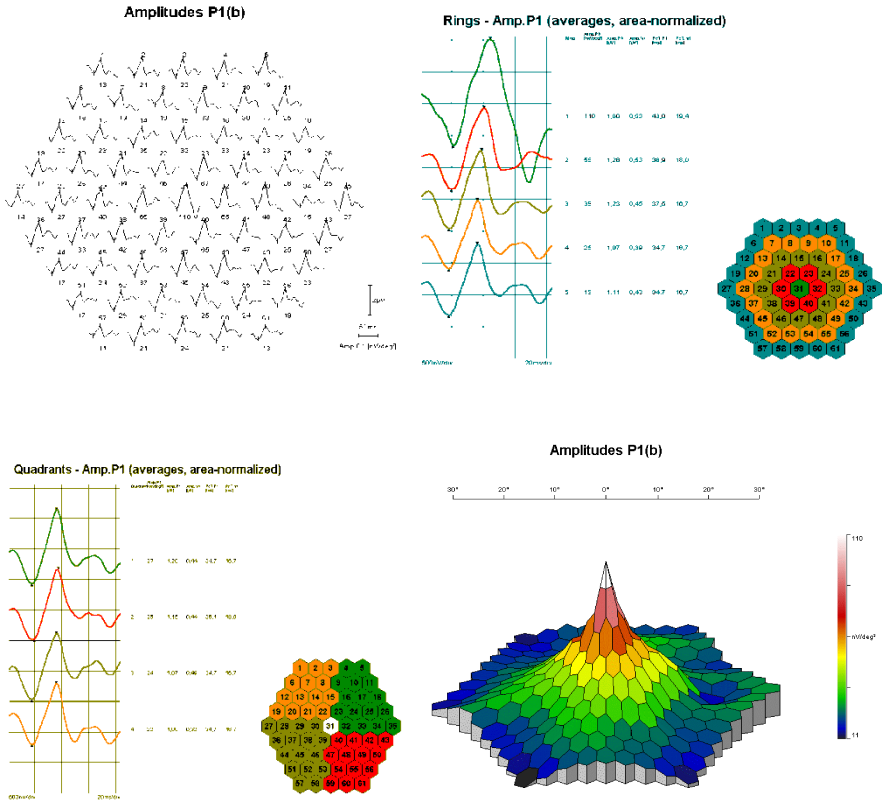

Figure 3. Sample of mfERG trace arrays (field view) with 61 elements *(top left)*, group averages *(top right),* quadrants *(bottom left)*, topographic (3-D) response density plots associated with trace arrays *(bottom right)*.

For the normative values of mfERGs see Table 2.

	Mean	Median	SD	Percentiles 05	Percentiles 95	CV
Centrum	127,54	125,00	25,93	96,06	211,00	0,20
Ring 2	64,56	66,00	10,03	47,50	80,90	0,16
Ring 3	41,98	41,00	6,16	31,30	51,90	0,15
Ring 4	29,65	30,00	4,68	20,50	37,90	0,16
Ring 5	25,68	24,00	5,72	17,20	35,00	0,22
Quadrant 1	34,31	33,50	6,26	26,53	45,90	0,18
Quadrant 2	30,68	30,00	4,91	23,04	40,85	0,16
Quadrant 3	31,28	30,00	5,24	24,00	41,90	0,17
Quadrant 4	31,60	29,00	6,69	22,04	43,00	0,21

Table 2. Normative mfERG data in the group of healthy subjects with good vision. (SD: standard deviation, CV: coefficients of variability)

3.2.3. Pattern electroretinography (PERG)

PERGs were studied in 68 controls, healthy subjects with good vision. Their mean age was 34.88 ± 14.77 years, with a range of 10-72 years.

The pupils of the volunteers were not dilated before examinations.

DTL electrodes were routinely used as active electrodes. Gold cup electrodes 5 mm in diameter were used as reference electrodes pasted 1 cm laterally from the ipsilateral orbital rim, and as ground electrodes, placed over the midline of the forehead (Fz). Sampling rate was 1000 Hz. Impedance was kept below 5 kΩ.

The viewing distance was 33 cm. Subjects had normal or corrected-to-normal VA (1.0). Binocular stimulation was applied.

Black and white checkerboard patterns with check sizes of 30' of visual angle served as the stimulus. The VF extent of the stimulus display was 12º vertically and 16º horizontally. The contrast of the patterns was 97%. The reversal rate was 2 Hz. Filters were set to 1 and 100 Hz. Two hundred responses were averaged. To test trial to trial variability all tests were repeated in the same session after a break of 2 min.

The PERG waveform consists of a small initial negative component with a peak time of approximately 35 ms, N35, which is followed at 45–60 ms by a much larger positive component (P50). This positive component is followed by a larger negative component at 90–100 ms (N95).

For a representative PERG recording see Figure 4 below.

Figure 4. A normal PERG recording. Abscissa: time in ms, ordinate: amplitude in μV. Calibration: 6.2μV, 25 ms

The implicit time of the peaks and the amplitude values of the N35/P50 and P50/N95 were determined. The implicit time was measured from the onset of the contrast reversal to the peak of the component. The P50 amplitude of the PERG was measured from the trough of N35 to the peak of P50. In some patients the N35 was poorly defined; in these cases N35 was replaced by the average baseline between time zero and the onset of P50. The N95 amplitude was measured from the peak of P50 to the trough of N95.

Normative PERG data are shown in Table 3.

	Mean	Median	SD	Percentile 05	Percentile 95	CV
N35 latency (ms)	30,34	30	1,37	28,3	33	0,05
P50 latency (ms)	52,28	52	1,77	50	56	0,03
N95 latency (ms)	93,69	94	5,53	83,3	101	0,06
N35-P50 amplitude (µV)	7,94	7,98	1,97	4,78	11,11	0,25
P50-N95 amplitude (µV)	10,56	10,6	2,38	5,91	14,44	0,23
RCT2	21,03	20,5	4,37	11,65	31,35	0,21
RCT3	50,52	51	4,45	40,2	57,4	0,09

Table 3. Normative data to PERG. (SD: standard deviation, CV: coefficients of variability, RCT: retino-cortical time, RCT2 is the difference of the VEP N75 amplitude and the PERG P50 amplitude, RCT3 is the difference of the PVEP P100 amplitude and PERG P50 amplitude)

3.2.4. Pattern visual evoked potential (PVEP)

To determine of normal values of VEP 50 control subjects were tested. Their mean age was 38.48 ± 16.14 years, with a range of 7-72 years.

The pupil of the volunteers was not dilated before examinations.

VEPs were recorded through gold cup electrodes. The recording electrode (gold cup) was placed on the Oz site, the reference electrode on the Fz site. The ground electrode was placed on the Fpz site. Sampling rate was 1000 Hz. Impedance was kept below 5 kΩ.

The viewing distance of the black-and-white checkerboard stimulus pattern was 33 cm. Subjects had normal or corrected-to-normal VA (1.0). Monocular stimulation was applied. The VF extent of the stimulus display was 12º vertically and 16º horizontally. The check sizes were 20 and 40'of visual angle. In cases of simultaneous recording of PVEP and PERG the check size was 30'. The contrast was 97%. The reversal rate of the stimulus was 0.9 Hz. Filters were set between 1 and 100 Hz. One hundred responses were averaged. To test trial to trial variability, all tests were repeated in the same session after a break of 2 min.

For a standard healthy VEP recording see Figure 5 below.

Figure 5. A normal VEP recording. VEPs are presented as continuous lines. Abscissa: time in ms, ordinate: amplitude in μV. Calibration: 6.2 μV, 25 ms.

The PVEP waveform consisted of three peaks: the N75, P100 and N135 peaks. For the characterization of PVEPs the N75, P100 and N135 latencies and the N75/P100 and P100/N135 amplitudes were used.

The normative data of PVEP are presented in Table 4.

VEP 64'	Mean	Median	SD	Percentile 05	Percentile 95	CV
N75 latency (ms)	70,64	71,00	4,95	61,40	79,00	0,07
P100 latency (ms)	104,41	105,00	5,53	95,30	114,00	0,05
N135 latency (ms)	145,15	146,00	16,30	120,00	177,20	0,11
N75P100 amplitude (μV)	13,37	13,10	4,92	4,32	22,70	0,37
P100N135 amplitude (μV)	13,35	12,10	5,08	6,48	23,33	0,38
N135-N75 latency differences (ms)	74,44	72,00	17,22	48,20	108,10	0,23
VEP 30'						
N75 latency (ms)	73,85	74,00	5,39	63,00	83,00	0,07
P100 latency (ms)	104,54	105,00	4,73	96,30	113,00	0,05
N135 latency (ms)	142,54	146,00	12,83	122,00	165,00	0,09
N75P100 amplitude (μV)	13,82	13,80	4,94	5,80	21,17	0,36
P100N135 amplitude (μV)	15,23	14,10	5,63	8,57	29,51	0,37
N135-N75 latency differences (ms)	68,69	68,00	13,96	47,00	91,00	0,20

Table 4. Normative data to PVEP stimulation. (SD: standard deviation, CV: coefficients of variability)

4. Clinical studies

4.1. Clinical studies I.: Multifocal ERG reveals several patterns of cone degeneration in retinitis pigmentosa with concentric narrowing of the visual field

MfERGs of 86 eyes of 43 patients with RP were analyzed. The diagnosis was based on the major clinical symptom - night blindness - and VF narrowing, the ophthalmoscopic picture and the characteristic ERG alterations. Mean age of the patients was 31.44 years, within the range of 6-64 years.

Inclusion criteria were as follows: VA at least 0.2 in the worse eye (allowing fixation on the central cross in the stimulus pattern) and a residual VF of at least 5-10º as detectable

by the Goldmann perimetry with the III.4 white stimulus). None of these patients had recordable ERG by the standard full field method.

The clinical characteristics of the patients are listed in Table 5.

	Patients									Eyes		
	n	**Gender**		**Genotype**		**Age at Testing**		**Visual acuity**		**n**	**Visual Field**	**n**
Total	43	Male	14	U	7	Mean	31.44	Mean	0.63	86	5-10º	19
				AD	10	Range	6-64	Range	1.0-0.2		10-15º	33
		Female	29	AR	12						15-20º	34
				S	14							
Group I	14	Male	2	U	4	Mean	28.64	Mean	0.86	28	5-10º	1
				AD	5	Range	14-55		1,0-0.8	20	10-15º	9
		Female	12	AR	3				0.7-0.5	8	15-20º	18
				S	2				<0.4	0		
Group II	16	Male	7	U	2	Mean	34.37	Mean	0.65	32	5-10º	2
				AD	3	Range	11-55		1,0-0.8	13	10-15º	16
		Female	9	AR	4				0.7-0.5	12	15-20º	14
				S	7				<0.4	7		
Group III	13	Male	5	U	1	Mean	31.33	Mean	0.4	26	5-10º	16
				AD	2	Range	6-33		1,0-0.8	3	10-15º	8
		Female	8	AR	5				0.7-0.5	12	15-20º	2
				S	5				<0.4	11		

n, number of patients or eyes in the corresponding group. U, Usher syndrome; AD, autosomal dominant; AR, autosomal recessive; S, simplex.

Table 5. Clinical data of the 43 patients.

MfERGs were recorded according to the standard method described in Chapter 3.2.2.

The mfERG alterations were analysed by trace array, ring and quadrant analysis. The results were compared to control data from 21 normal volunteers. Data were analyzed with a two-way ANOVA for group and for category. When ANOVA showed significant differences, post-hoc analysis was performed with the Dunnett test. $P < 0.05$ was considered significant.

The three dimensional presentation generally showed a characteristic central peak surrounded by very small responses in this disease. However, 13 of the 43 patients had not even a central peak. On the basis of the best response density of the mfERGs, the patients were divided into three groups.

Patients in G*roup I* (*n*=14) presented typical mfERGs and typical VF constrictions on both sides. The area of best responsiveness was found to be the 31st hexagon, producing a central peak surrounded by low responses depending on the severity of VF constriction. However, even if the peripheral rings had almost undetectable kernels, one or two 'good'

responses were almost obtainable in the trace arrays (e.g. 10, 11 or 51). Furthermore, in spite of the characteristic central peak, the mean amplitude values of the 31. kernels were significantly subnormal as compared to the normal control values (mean: 43,06 nV/deg^2, range: 17,2-82,2 in patients with RP, and 109, 62 nV/deg^2, range 51,3-136 in controls) (see Figure 6). The differences between these two variables were significant (P<0.00001). In both the control subjects and the patients with RP, the amplitudes of the responses declined rapidly toward the outer rings.

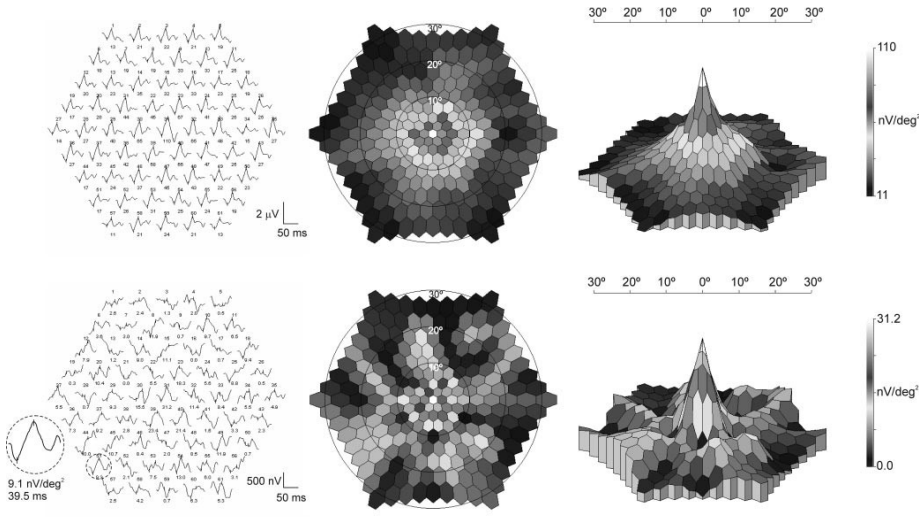

Figure 6. (*top*) mfERG recordings of a control, healthy subject and of a RP patient in group I (*bottom*). The best response density was found in the central hexagon, presenting as a central peak surrounded by very low responses in the three-dimensional presentation. *Left*: trace arrays (note the differing calibration). In the *bottom left* corner, kernel 53 (*encircled*) is magnified. The density of the response and the latency of its P1 wave are indicated below it. *Middle*: two-dimensional presentations; *right*: three-dimensional presentations with calibrations.

The severity of the mfERG alterations did not correlate well with the age of the patients. Some young patients had a low central peak of the mfERG, and there were older patients with only a mild sensitivity loss. Their mean VA was 0.86, and only three patients had a VA of 0.5 in the worse eye (Table 5).

In *Group II* (*n*= 16) the best response was found in the 31st position of the trace array on only one side. In the fellow eye, the best response density appeared in an eccentric position (Figure 7). This alteration could not be a consequence of a fixation problem, as the fusion phenomenon keeps the eyes motionless during binocular stimulation. No laterality differences were found in the refraction or in the VA. The ophthalmoscopic picture of the

macular area was similar in both eyes without any abnormality such as cystoid macular oedema or epiretinal membrane. No history of strabismus or other eye disease could be responsible for these differences. Latent exo- or esotropia was excluded by careful orthoptic examination.

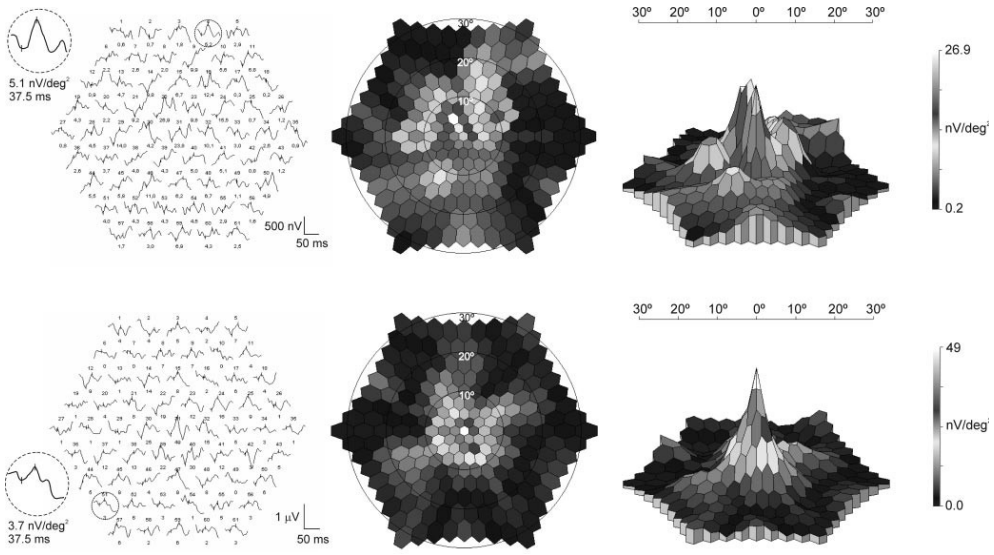

Figure 7. MfERG recordings of an RP patient in group II. *Top*: mfERGs of the eye with eccentric fixation; *bottom*: mfERGs of the fellow eye with central fixation. *Left*: trace arrays; *middle*: two-dimensional presentations; *right*: three-dimensional presentations with calibrations. To the *left* of each trace array, the kernel encircled is magnified. The response density of the response and the latency of its P1 wave are indicated below them.

In cases where the area of best responsiveness was found in an eccentric position, we repeated the stimulation monocularly as well. In both conditions, the best responses were found outside the central position. In this group, the averaged mean amplitudes of the responses in the first ring of the mfERGs were lower than in group I, although some eyes had a very good central peak. Accordingly, we analyzed the mfERG findings of this group in two subgroups, depending on the site of the best responses. Group II.A comprised the mfERGs of the eyes with a central response, and group II.B of those of the fellow eyes with an eccentric best position. The amplitudes of the responses in the first ring of the group II.A eyes (mean, 47.41 nV/deg^2) were almost the same as those in group I. The eyes with eccentric best responses (group II.B) produced lower amplitudes in the first ring (mean, 24.36 nV/deg^2). No significant side differences between the two eyes were found in the amplitudes of the third, fourth, and fifth rings or in the four quadrants.

The patients in group II had a mean VA of 0.65. Altogether, 25 of the 32 eyes exhibited VA better than 0.5 (Table 5.).

The patients in *Group III* (*n*=13) presented no central peak in the mfERG on either side. These cases were classified in earlier studies as 'undetectable mfERGs' or as artefacts. However, in some parts of the trace array, we found satisfactorily intact responses in all these patients (Figure 8.). In these plots, the best responses were found at rather variable sites (e.g., hexagons 17 and 47). In some cases, there were two or three peaks of low amplitude in the three-dimensional presentation of scalar products, making them 'uneven', 'patchy' in appearance, or 'unrecordable'. The mean amplitude in the first ring of the mfERGs in this group was rather low (19.28 nV/deg^2). The appearance of some characteristic, though small, responses convinced us that these mfERG recordings could not be attributed merely to artefacts or noise. Repeated examinations gave almost corresponding results.

It is noteworthy that these patients also had satisfactory VA (0.9–0.2, mean, 0.4). Three eyes had a VA of 0.9, and 12 one had 0.5 or better (0.7– 0.5).

We did not find any relationship between our groups on the basis of the mfERG recordings and the heredity pattern of the patients.

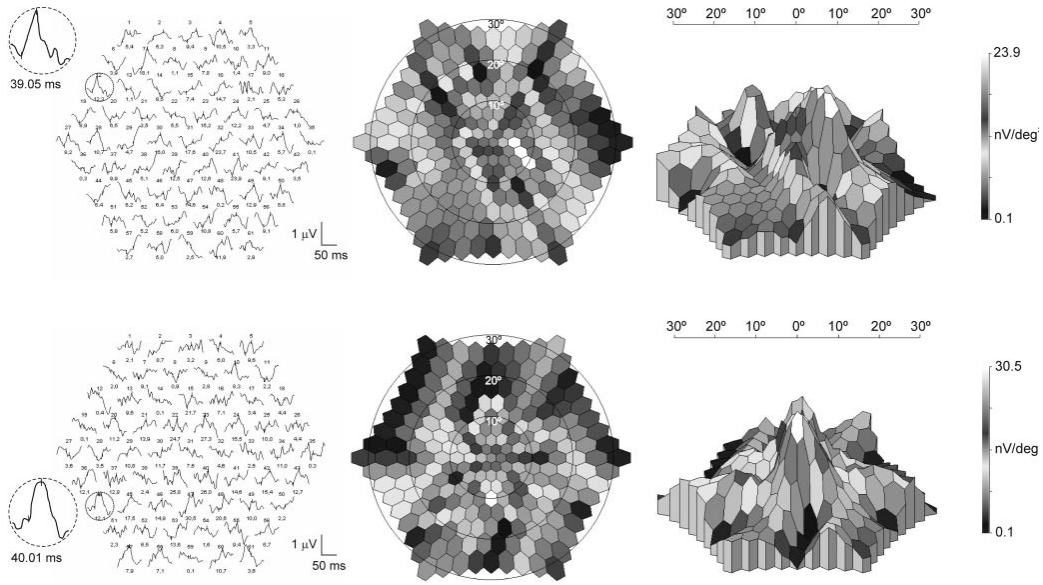

Figure 8. MfERG recordings of the right eye (*top*) and left eye (*bottom*) of a patient with RP in group III. *Left*: trace arrays; *middle*: two-dimensional presentations; *right*: three-dimensional presentations with calibrations. To the *left* of each trace array, the kernel encircled is magnified. The density of the response and the latency of its P1 wave are indicated below them. Values of the fourth and fifth rings are omitted. These data were not informative because the amplitudes were very low.

4.2. Clinical studies II: Pattern-reversal electroretinograms and visual evoked potentials in retinitis pigmentosa

To determine PERG and VEP in RP patients 106 eyes of 53 patients with different inheritance and durations of RP were analyzed. The age-matched normal values were calculated by taking into account the PERG parameters of 114 eyes of 57 subjects and the PVEP parameters of 146 eyes of 73 subjects with good vision and without any ophthalmological or systemic disease. The clinical characteristics of the patients are summarized in Table 6.

	Inheritance	n	Age at the onset of the disease (years)	n	Age at the examination (years)		Visual acuity (eyes)	n	VF defect (eyes)	n
Group I	AD	5	0–20	10	Mean	38.76	Mean: 0.71	34		34
n = 17	U	3	20–30	3	Range	14–64	1.0–0.8	16	5º–10º	4
Male 4	AR	3	30<	4			0.7–0.5	8	10º–15º	6
Female 13	S	6					0.4–0.2	10	15º–20º	24
Group II	AD	9	0–20	14	Mean	26.75	Mean: 0.85	32		32
n = 16	U	2	20–30	1	Range	12–70	1.0–0.8	8	5º–10º	2
Male 4	AR	4	30<	1			0.7–0.5	21	10º–15º	12
Female 12	S	1					0.4–0.2	3	15º–20º	18
Group III	AD	10	0–20	12	Mean	35.5	Mean: 0.59	40		40
n = 20	U	2	20–30	4	Range	16–52	1.0–0.8	2	5º–10º	16
Male 13	AR	6	30<	4			0.7–0.5	26	10º–15º	4
Female 7	S	2					0.4–0.2	12	15º–20º	20

AD Autosomal dominant; U Usher syndrome; AR Autosomal recessive; S Simplex

Table 6. Clinical characteristics of the patients

To determine PERG alterations, the N35, P50 and N95 peak times and the N35/P50 and P50/N95 amplitudes were measured. For the characterization of PVEPs the N75, P100 and N135 implicit times and the N75/P100 and P100/N135 amplitudes were used. The waveform alterations of PVEP were regarded as having double P100 peaks if two positive waves appeared in this interval with a negativity of at least 1 μV. The amplitudes between the larger positive peak and N135 (Pmax/N135) were used to express the magnitude of the deflection, independently of whether P1 or P2 was the larger. The broadness of the response was characterized by the latency differences between N135 and N75.

Statistical analysis was performed only on recordable, reproducible responses. Data are presented as means ± SD. The results were analyzed by a one-way ANOVA. Subsequent analysis was performed using Newman-Keuls test. A p-value less than 0.05 was considered significant. Data were analyzed with STATISTICA 7.1. software (Statsoft Inc., Tulsa, OK).

Seventeen of the 53 patients (32%) yielded recordable, reproducible PERGs. Of these 17 patients, 4 yielded reproducible PERGs from only one eye. Both the N35/P50 and

P50/N95 amplitudes of the PERGs were significantly smaller than those of the controls (Table 7.). We failed to record a normal PERG from any of the patients.

All 53 patients yielded PVEPs which fitted the criteria of reproducibility, though characteristic alterations were detected in some cases. Depending on the type of these alterations, we divided the patients into three groups (Figure 9.). No statistical correlation was found between this division and the age or the duration of RP or the extent of the VF defect in the patients.

The PVEPs in the three groups exhibited certain characteristics as follows.

All the patients in *Group I* (n = 17; 32%) had PVEPs with a normal shape. These PVEPs revealed significantly smaller amplitudes in comparison with the age matched control group. The peak time of the P100 components was slightly delayed in a few cases, but no longer than 120 ms. The N135 peaks were at times slightly delayed too, but this alteration did not reach the level of significance (Table 8.). The interindividual variability of the amplitude of the PVEPs was rather large.

		RP patients		**Controls**	
		Right eye n=15	**Left eye n=15**	**Right eye n=57**	**Left eye n=57**
N35	Mean ± SD	35.00 ± 4.12	35.38 ± 7.65	30.02 ± 1.22	30.16 ± 1.94
	Range	27.0–43.0	20.0 - 49.0	27.0 - 34.0	22.0 - 35.0
P50	Mean ± SD	60.64 ± 6.55*	60.92 ± 13.08*	51.72 ± 1.72	51.74 ± 1.65
	Range	50.0 - 71.0	38.0 - 98.0	47.0 - 56.0	49.0 - 56.0
N95	Mean ± SD	103.73 ± 13.35	95.93 ± 12.06	92.86 ± 5.37	92.93 ± 5.18
	Range	93.0 - 146.0	70.0 - 116.0	81.0 - 107.0	81.0 - 102.0
N35/P50	Mean ± SD	2.16 ± 0.98*	2.25 ± 2.21	9.55 ± 3.82	9.75 ± 4.24
	Range	1.1 - 4.1	0.7 - 9.7	4.1 - 24.1	4.2 - 29.6
P50/N95	Mean ± SD	3.39 ± 1.89*	2.78 ± 2.31	12.78 ± 4.67	12.96 ± 5.59
	Range	1.3 - 9.0	1.3 - 10.5	5.7 - 29.4	5.8 - 37.6

* Denotes significant (P\0.05) differences in comparison to controls

Table 7. Implicit time and amplitude values of PERGs in RP patients (left) and those of healthy controls (right)

There was no direct correlation between the decrease in amplitude and the age of the patient or the amplitude and the estimated duration of the disease. In this group, subnormal PERGs were recorded in 14 eyes, while they were extinguished in 20 eyes.

The VF constriction assessed via the Goldmann perimeter varied in severity (5º–20º). The upper and lower parts of the field in these patients displayed almost the same degree of constriction. In some cases, a 5º–10º VF crescent was preserved in the temporal lower part of the far-peripheral field, close to 90º.

In *Group II* (n = 16; 30%), the PVEPs had a characteristic, bifid pattern and the recordings demonstrated well-defined, doubled P100 peaks (P1 and P2). The two

components of P100 were separated by about 50 ms. In 6 patients P1 was the larger, while in another 6 cases P2 was the larger, and in 4 cases there was no difference in amplitude between the two peaks. The double peak, or 'W' form, of the P100 peak may lead to confusion in the interpretation and in the statistical analysis. It appeared inappropriate to presume that one or the other was 'the true' P100. To express the absolute size of the deflection, not only the N75/P100 amplitude, but also the Pmax/N135 components were determined. The decrease in amplitude and the lengthening of the implicit time of P1 were moderate, but both values revealed a significant difference as compared to the controls (Table 8.). However, the P2 latencies were rather long and the N135 latencies were greatly delayed. In several cases, the N135 latency was longer then 200 ms. The inter-peak time of the negative components (N135 and N75) were significantly longer than those in the controls (Figure 9.). The Pmax/N135 amplitudes were significantly larger than the N75/P100 amplitudes in this group and than the P100/N135 amplitudes in the two other groups of our patients. This resulted in the characteristic asymmetrical shape of the curves. Furthermore, the N135/N75 latency differences were significantly larger than those of the controls and those observed in Group I.

Subnormal PERGs were recorded in 14 eyes, while the PERGs were extinguished in 18 cases. Similarly to Group I, Goldmann perimetry revealed a concentric narrowing of the field, with preserved central part. Several patients exhibited the substantial narrowing in the upper hemifield that approached the central 5º but never involved it. In 14 eyes of the 16 patients, 5–15º of the fields was intact; in the remainder (18 eyes), the central 20º of the visual field was preserved.

All the recordings in *Group III* (n = 20; 38%), (40 eyes of 20 patients) revealed a serious impairment, albeit they were reproducible. They had a delayed implicit time, and most of the recordings had decreased amplitudes. No true doubled peaks with P1 and P2 could be separated, although the waveform was broad and sometimes very flat. Not only the P100, but also the N75 and N135 latencies were significantly delayed. It is worth noting that the latency differences between the N135 and N75 peaks were significantly longer than in the normal controls.

There were no strict correlations between the VA and the PVEP parameters or VF loss, since some patients in this group exhibited sufficient VA. However, the mean visual acuity in Group III was only 0.4. Only 4 eyes of 2 patients yielded recordable, reproducible PERGs. Upon Goldmann perimetry, the field in 20 eyes was constricted up to 15–20º, while in the rest there was only a field-remnant of 5º to 10º.

The mean amplitudes and their variability in the three groups are presented in Table 8.

	Group I		Group II		Group III		Control	
	Right eye	**Left eye**	**Right eye**	**Left eye**	**Right eye**	**Left eye**	**Right eye**	**Left eye**
N75	75.1 ± 6.47	75.8 ± 6.47	73.6 ± 6.37	75.6 ± 8.66	89.0 ± 15.36*	87.1 ± 4.67*	73.3 ± 6.18	74.2 ± 6.09
Range	63.0 - 87.0	57.0 - 88.0	58.0 - 84.0	58.0 - 90.0	66.0 - 118.0	59.0 - 110.0	60.0 - 85.0	60.0 - 84.0
P100	105.2 ± 6.46	108.5 ± 7.71	109.4 ± 7.51*	108.9 ± 7.62*	134.9 ± 15.58*	136.5 ± 15.84*	103.0 ± 5.95	103.6 ± 5.44
Range	95.0 - 117.0	96.0 - 123.0	97.0 - 120.0	93.0 - 120.0	120.0 - 175.0	114.0 - 175.0	90.0 - 114.0	90.0 - 117.0
P2100	–	–	158.4 ± 22.05	156.5 ± 24.54	–	–	–	–
Range	–	–	132.0 - 201.0	122.0 - 200.0	–	–	–	–
N135	147.3 ± 13.62	155.0 ± 18.90	207.4 ± 37.19*	203.0 ± 34.64*	199.9 ± 24.23*	204.6 ± 25.21*	142.1 ± 13.72	141.9 ± 13.49
Range	120.0 - 170.0	123.0 - 180.0	151.0 - 266.0	151.0 - 253.0	162.0 - 236.0	160.0 - 255.0	121.0 - 180.0	120.0 - 174.0
N75/P100	6.4 ± 3.05*	7.5 ± 3.83	8.3 ± 2.47*	7.5 ± 2.94*	5.1 ± 1.81*	4.6 ± 1.43*	14.4 ± 6.63	14.2 ± 6.77
Range	2.1 - 11.9	1.6 - 14.9	3.7 - 11.7	2.5 - 14.1	2.8 - 9.2	1.9 - 7.7	3.1 - 34.5	2.2 - 34.3
P100/N135	6.9 ± 3.03*	8.1 ± 3.61*	11.5 ± 4.01*	11.8 ± 4.54*	5.8 ± 1.89*	5.7 ± 2.45*	15.4 ± 6.45	15.5 ± 6.12
Range	1.7 - 11.9	1.8 - 14.5	5.7 - 19.5	3.8 - 19.5	1.9 - 8.7	1.0 - 10.2	2.8 - 35.7	6.9 - 35.9
N135-N75	72.2 ± 13.46	79.2 ± 19.37	133.6 ± 34.52*	127.5 ± 30.23*	110.9 ± 22.46*	117.5 ± 25.03*	68.9 ± 14.64	67.7 ± 14.81
Range	51.0 - 101.0	52.0 - 123.0	80.0 - 186.0	80.0 - 169.0	75.0 - 152.0	0	41.0 - 113.0	42.0 - 103.0

For Group II P100/N135 denotes Pmax/N135 values

- Denote significant (P\0.05) differences in comparison to controls

Table 8. Amplitude and latency values (mean ± SD) of PVEPs recorded in the three groups of RP patients and in controls

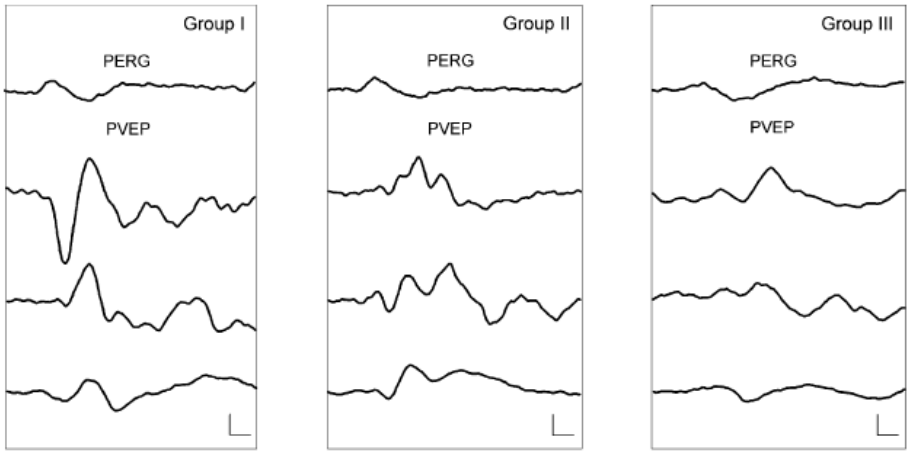

Figure 9. Electrophysiological recordings in the three groups of RP patients. *Top:* PERG curves in the respective groups. The bottom three curves depict three representative PVEP recordings in each group. PVEPs are presented as continuous lines. Calibration: 6.2 lV, 25 ms.

4.3. Clinical studies III.: Melanoma associated retinopathy (MAR) syndrome

Case history and clinical symptoms of a monocular case with MAR syndrome is presented.

A cutaneous malignant melanoma was removed from the left leg of a 45-year-old woman in 1992. Because a systematic search revealed no metastasis, no further therapy was administered.

One evening in January 2000, she suddenly experienced difficulty seeing in dark conditions through her right eye, which greatly interfered with her stereovision. She also reported shimmering lights that fluctuated in brightness.

Because an ophthalmological examination demonstrated good VA and no fundus alterations, the patient's complaints were judged to be of psychic origin. Four months later, a metastatic cutaneous melanoma was removed from her left leg. She underwent chemotherapy and was referred to our electrophysiological laboratory because of her persisting visual complaints.

She still had a best-corrected VA of 20/20 on both side. Static perimetry (Octopus) revealed a marked VF constriction and a general depression of light sensitivity in the right eye. The left eye exhibited no perimetric alterations (Figure 10.).

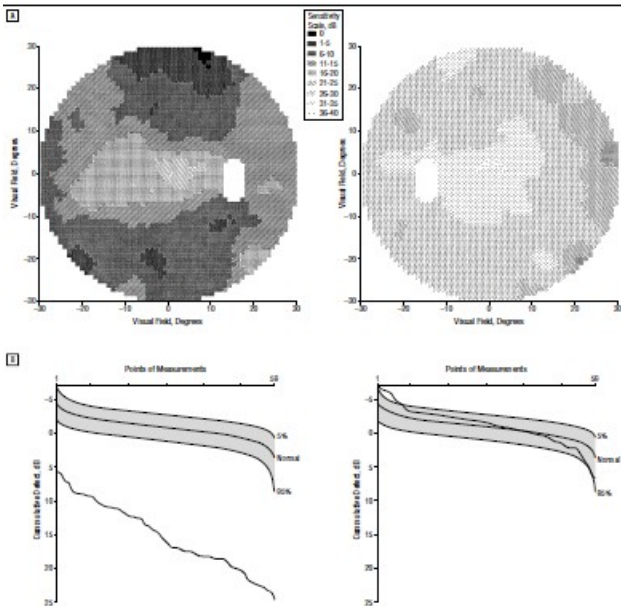

Figure 10. A, VF of the right eye (left) and left eye (right) estimated using Octopus perimetry. The x- and y-axes represent dimensions of the VF in degrees. B, Cumulative defect curves (Bebie curve) from the 59 central points in rank order cumulative sensitivity distribution.

The single-flash ERG showed a markedly decreased scotopic response in the right eye, whereas maximal-intensity stimulation elicited a typical ERG that showed no abnormalities, a selective b-wave depression with a preserved a wave (Figure 11.). Both the scotopic rod-isolated response and the maximal response in the left eye were in the normal range. The averaged ERG and OPs were greatly impaired in the right eye but normal in the left eye.

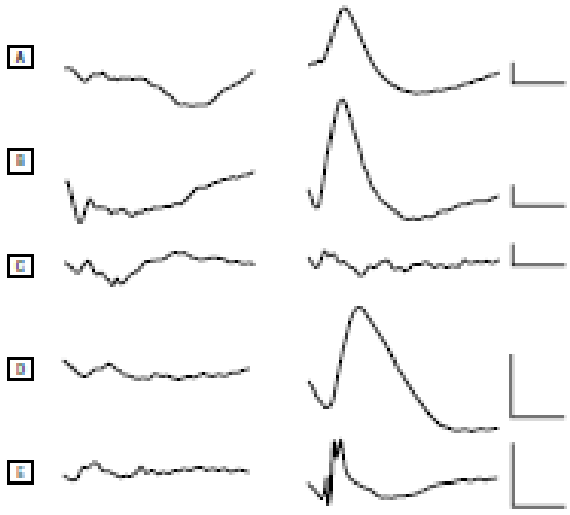

Figure 11. Electrophysiological recordings from the right eye *(left)* and left eye *(right)* of the patient.
A, Scotopic, rod-isolated response.
B, Maximal, dark-adapted response.
C, Electroretinographic (ERG) response to red flash. D, Averaged ERG response to 50 blue flashes. E, Averaged OPs to 50 blue flashes. Calibrations: 50 μV; 100 ms.

Serum immunochemistry revealed strong binding to retinal bipolar cells, similar to that of a known patient with MAR. This result supported the diagnosis of MAR, so our case was the first monocular case of this disease.

Five control electrophysiological examinations together with perimetry and ophthalmoscopy showed no changes during the following 15-month observation period. Unfortunately, the patient developed agranulocytosis in July 2001 and died of pulmonary metastases and respiratory failure 1 month later. The family did not allow an autopsy.

4.4. Clinical studies IV.: Diseases with visual field narrowing

4.4.1. Clinical studies IV/A.: Electrophysiological findings in patients with nonarteritic anterior ischaemic optic neuropathy (NAION)

Beside VF testing (Goldmann kinetic perimetry), scotopic, photopic and flicker ERGs, mfERGs, PERG and VEP were performed for the objective evaluation of the severity of the functional loss in 8 NAION patients. The methods are described in Chapter 3.

The diagnosis was based on the history and symptoms: a sudden visual loss or VF loss, optic disk oedema followed by pallor of the disk, a relative afferent pupillary defect, altitudinal VF defect with narrowing the isopters (in all four retinal quadrants).

Histories, clinical conditions and suspected predisposing factors are listed in Table 9.

An intracranial cause of the visual loss was excluded by careful neurological examination, intracranial and orbital MRI and CSF analysis. MRI revealed small white matter lesions in two patients (Cases 1 and 2). However, these could not be linked to the visual loss. Other pathologies of disk oedema such as vasculitis, syphilis, borelliosis, herpes

simplex, etc. were excluded by serological and immunological tests. Colour Doppler ultrasonography ruled out intracranial circulatory disturbances.

The electrophysiological results are presented in the form of individual recordings in 3 patients in Figure 12.

Patient	Sex	Age (yrs)	How long ago 1. Eye[a] 2. Eye[b] (duration) Was attacked	Optic disk at attack	Visual acuity at examination	Optic disk at attack	Visual field at examination	Underlying disease
Case 1	M	66	12 yrs[a]	1.0 D disk oedema	1.0	Pale	Temporal upper constriction	Hypertension (20 yrs)
			2 yrs[b]	2.0 D disk oedema + haemorrhage	1.0	Pale	Nasal constriction	Diabetes mellitus (2 yrs)
Case 2	M	62	6 yrs[a]	3.0 D disk oedema	0.95	Pale	Nasal lower constriction	Hypertension
			8 mts[b]	2.0 D disk oedema + haemorrhage	1.0	Pale	Nasal lower constriction	
Case 3	F	52	12 yrs[a]	3.0 D disk oedema	1.0	Milky-white	50–20º constriction	Cardiac disease (12 yrs)
			6 yrs[b]	2.0 D disk oedema	0.85	Milky-white	Nasal lower constriction	
Case 4	F	59	15 yrs[a]	1.0 D disk oedema	0.15	Milky-white	Nasal lower constriction	Type 2 diabetes mellitus (15yrs)
			13 yrs[b]	Blurred margin	0.15	Pale	Nasal lower constriction	
Case 5	F	55	11 yrs[a]	Not visible (cataract)	0.04	Milky-white	Not detectable	Type 2 diabetes mellitus (15yrs) cataract
			7 yrs[b]	Blurred margin	0.1	Pale	Concentric narrowing to 10º	
Case 6	F	36	5 yrs[a]	1.0 D disk oedema	0.15	Milky-white	Concentric narrowing to 20º	Type 2 diabetes mellitus (12yrs)
			4 yrs[b]; two	1.0 D disk oedema attacks in 2 mts	Light perception	Milky-white	Not detectable	
Case 7	M	64	8 days[a]	1.0 D	0.01	1.0 D disk edema	Not detectable	No underlying disease
			Normal[b]	Normal	1.0	Normal	Normal	
Case 8	M	68	3 yrs[a]	2.0 D disk oedema	0.02	Milky-white	Concentric narrowing to 10º	No underlying disease
			Normal[b]	Normal	1.0	Sector-type Decoloration	Normal	

Abbreviations. yrs: years, mts: months, M: male, F: female.
a The eye that suffered the first attack.
b The eye that was afflicted secondarily (or not), together with the time passed since the attack.

Table 9. Clinical data of the 8 patients (Cases 1–8)

VEPs revealed a serious deterioration in most of the patients. This was especially marked in 3 cases (Cases 4, 5 and 6) where diabetes mellitus was the underlying disease. All of them had rather poor VA (Figure 12C). Similarly, the VEPs showed a considerable amplitude reduction and prolonged P100 peak time upon stimulation of the impaired eye in the two monocular cases (Cases 7 and 8; Figure 12D). A prolonged P100 implicit time was also the characteristic VEP alteration in the 3 patients with hypertension (Cases 1, 2 and 3;

Figure 12B). Interestingly, the VEPs of the non-involved eyes of the two monocular cases (Figure 12E) had delayed implicit time, too.

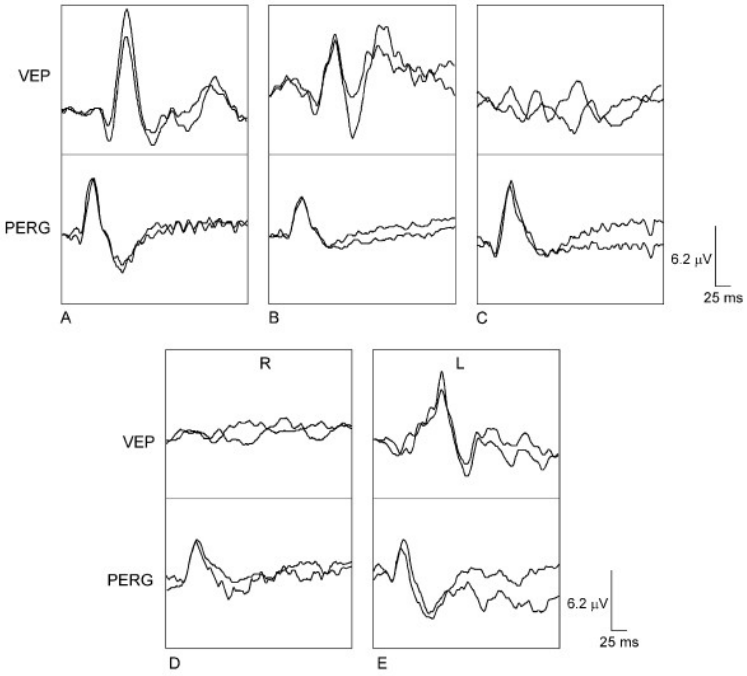

Figure 12. VEP (upper curves) and PERG recordings (lower curves; 30 in reversing checkerboards) upon stimulation of the right eye of a healthy, control subject (A), the right eye of Case 3, a patient with a VF defect and preserved VA (1.0) (B) and the right eye of Case 4, a patient with a serious visual loss (0.15) (C). D and E depict the electrophysiological recordings of the right and left eye, respectively, of Case 7, a patient with monocular affliction. The superimposed curves represent the results of subsequent recordings. Note the correlation between the VEP impairment and the deterioration of VA.

Unpaired *t* tests were carried out for statistical comparison. An age-matched group of 26 healthy individuals with good vision without any ophthalmological and systemic disease served as normal controls. Statistical comparison of the amplitude and implicit time values of the VEPs in patients with NAION and of the age matched normal controls revealed a significant increase in the implicit time of P100 ($P<0.001$) and a significant reduction in the amplitudes between N75 and P100 ($P=0.0001$) and in those between P100 and N135 ($P=0.0005$).

In contrast with the severe deterioration observed in the VEPs, the PERG recordings did not show major abnormalities. There were no statistical differences between the implicit time values of the patients and the controls, whereas some amplitude reduction was observed in most cases. Accordingly, statistical comparison of the amplitudes of the PERGs in patients and controls revealed significant differences (N35–P50: $P<0.0005$; P50–N95: $P<0.00003$). These

values, however, mostly lay in the range for the age matched normal group (Fig. 2). No selective P50–N95 amplitude reduction was found. The quotient of the P50–N95 amplitudes over the N35–P50 amplitudes of the patients (1.32±0.32) was not statistically different from that for the normal individuals (1.29±0.17). It was noteworthy, however, that the patients with diabetes mellitus and rather poor vision had better PERGs than those with hypertension. Patients with old age and long duration of hypertension had the most severe PERG alterations. No side differences were observed in the PERGs of the monocular cases.

In general, the most striking observation was that patients with poor VA did not have worse PERGs than those with good vision.

MfERGs had no obvious alterations in the patients.

4.4.2. Clinical studies IV/B.: Nonarteritic ischaemic optic neuropathy (NAION) in patients under 50 years of age

NAION is a rather frequent cause of sudden visual loss in elderly patients. However, we found three patients with diabetes, who had the first ischemic attack under the age of 50. We describe their case histories, clinical and electrophysiological findings.

For objective evaluation of the optic nerve function, visual evoked potentials (VEPs) were recorded (according to the methods described in Chapter 3.2.4.), whenever a recurrent event of visual loss or progression of visual impairment was reported.

Intracranial pathological alterations were excluded in all cases by careful neurological examinations, including CSF examination and cranial and orbital MRI testing (1.5 T; General Electric, Fairfield, CT, USA). Clinical laboratory tests for diseases that could cause optic neuritis or vasculitis (erythrocyte sedimentation rate, blood cholesterol level, complete blood count, antinuclear antibody, rheumatoid factor, C-reactive protein, venereal disease research laboratory test, herpes, toxocara, IgG in CSF) were routinely performed according to the general condition of the patient. The care of the patients' diabetes corresponded to international standards.

Case 1: A 35-year-old woman had suffered from insulin-dependent diabetes mellitus from the age of 22 years. Four years prior to this study, she noticed that the vision in her right eye had suddenly become blurred. A visual impairment was detected not only in the right eye, but also in the left. VA was 0.5 in the right eye and 0.4 in the left eye. The temporal parts of both optic discs were pale, and the nasal superior quadrant of the right disc was oedematous. Goldmann perimetry showed non-characteristic alterations consisting of an enlarged blind spot and a VF defect in the nasal inferior quadrant of the right eye and concentric narrowing of the isopters in the left eye (Figure 13A, B).

The patient's young age supported the presumptive diagnosis of multiple sclerosis. However, fat-suppressed, T1 and T2 sequenced brain and orbital MRI, somatosensory evoked potential and VEP, and CSF immune tests showed normal results. Intracranial circulation disturbances could be excluded by the normal results of colour Doppler examination of the internal carotids and the ophthalmic artery. Chemical analysis of the CSF and blood, serological tests for syphilis, borelliosis, herpes simplex infection and other immune tests yielded normal results. The presence of any other systemic diseases that might cause vasculitis was excluded as well. Nonetheless, the subject's neurologist put her on steroid treatment.

The next attack of visual impairment occurred 2 years later. VA in the patient's left eye decreased to 0.15. Repeated MRI examination failed to show any pathological signs. The patient was treated with steroids again, without any success. VA remained 0.15 in both eyes. VF defect covered the central part (Figure 13C, D).

One year later, the subject suddenly lost almost all vision in her left eye. The pupillary light reflex was sluggish and hardly elicitable.

No further recurrence of visual impairment was observed in the right eye. VA was 0.15 in the right eye and light perception in the left. Both optic nerve heads presented a milky-white appearance (Figure 14A, B). The VFs did not reveal any change in the defects in the right eye (peripheral constriction and central scotoma), while testing was not performed in the left eye because of the serious visual loss (Figure 13E, F). The patient underwent repeated orbital and cranial MRI and laboratory examinations that consistently provided evidence against multiple sclerosis, acute optic neuritis or vasculitis.

Case 2: A 50-year-old woman had diabetes mellitus for 12 years. Ten years prior to this study, at the age of 40 years, she noticed progressive visual disturbance in her right eye. The progression of the central visual loss lasted for only 3 days, but the narrowing of the VF continued for the following 2 weeks.

The subject's VA was 0.15 in the right eye and 1.0 in the left. The right optic disk had an oedematous swelling, whereas the left was normal. No signs of diabetic retinopathy were observed. The temporal part of the VF in her right eye was constricted to 35º, while the VF in the left eye remained normal.

Upon neurological examination, the MRI was found to be normal and the laboratory tests did not indicate any other pathology than diabetes and hypertension. Thiogamma (600 mg/day) was also administered because diabetic neuropathy was suspected to be the cause of the visual loss.

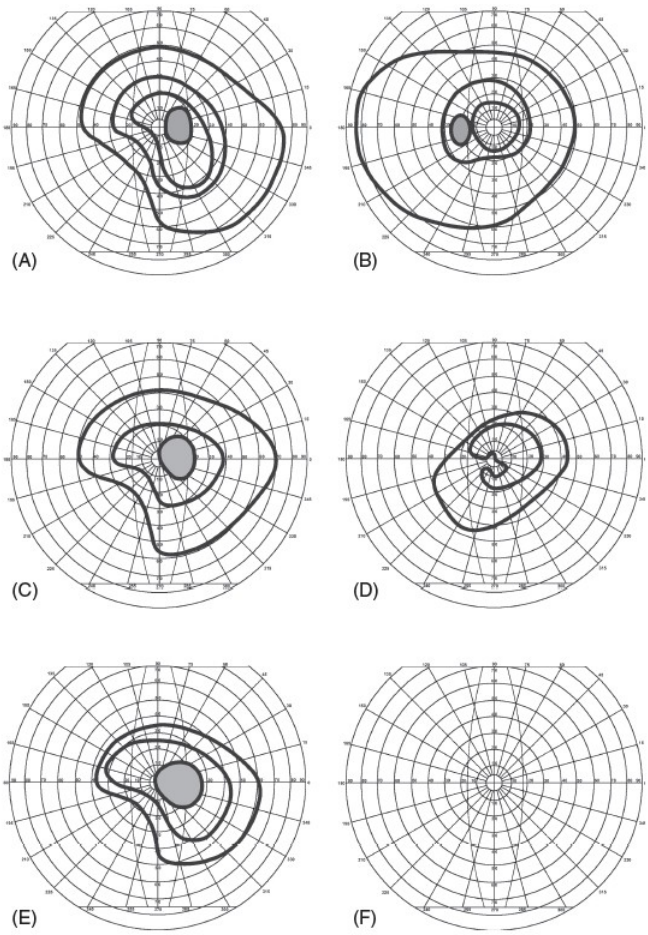

Figure 13. Progression of kinetic VF loss in the right and left eyes in case 1. (A, B) VFs after the first attack of NAION. Nasal inferior altitudinal narrowing of the isopters (tested with W4.5, W4.3 and W4.1 stimuli, respectively) and an enlarged blind spot are to be found in the VF of the right eye (A), while concentric narrowing of the isopters (W4.3 and W4.1) may be observed in the VF of the left eye (B). (C, D) Impairment of the VFs after the second attack: In the right eye (C) the enlarged blind spot has already engulfed half the temporal central area. In the left eye (D), further shrinkage of the isopters extends to two-thirds of the central visual area (W4.5, W4.2). (E, F) The VFs after the last attack of NAION. In the right eye (E), the centro-coecal scotoma covers almost the whole central area. In the left eye (F) VF testing was not possible because of the lack of fixation.

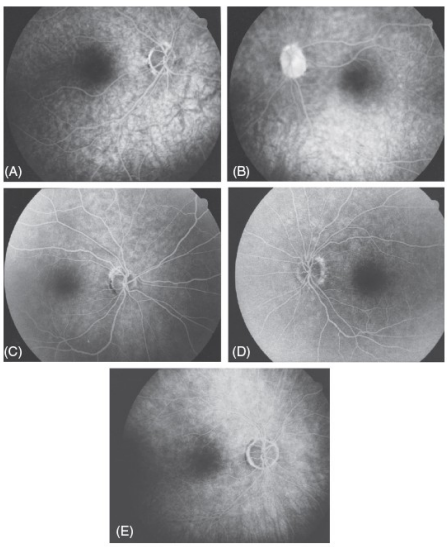

Figure 14. Fundus photographs by fluorescence angiography of the right (A) and left (B) eyes in case 1; of the right (C) and left (D) eyes in case 2, and of the right eye (E) in case 3. No photograph was taken of the left eye in case 3 because of the lack of fixation.

No change in VA or VF occurred during the subsequent year. Two years later, the patient suddenly lost vision in the left eye. Her ophthalmologist registered VA of 0.15 in the right eye and 0.08 (finger counting from a distance of 4 meters) in the left. The right optic disc was pale and the left was oedematous. The possibility of Foster–Kennedy syndrome, as a consequence of the intracranial pathology, was again excluded. No other symptoms have appeared since then. Her vision has never recovered: VA remains at 0.15 in the right eye and 0.1 in the left. Both optic nerve heads have become atrophic (Figure 14C, D). No diabetic retinopathy has developed. Her VF defects have changed during the past 2 years (Figure 15). No reproducible VEPs could be detected.

Case 3: A 51-year-old woman had non-insulin dependent diabetes mellitus for 12 years. At the age of 42, she noticed a progressive visual deterioration in her left eye, which at that time was ascribed to cataract formation. In the left eye, the retina was obscured by lens opacification. The VA was 0.4, which seemingly correlated well with the condition of her lens. Cataract surgery was performed. However, no improvement of vision was detected thereafter. Best corrected VA was 0.04. The head of the optic nerve was pale.

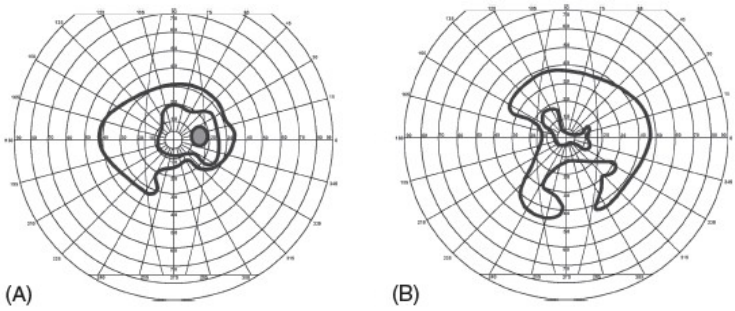

Figure 15. Kinetic VF impairments in the right (A) and left (B) eyes in case 2. Bilateral, relatively altitudinal, concentric VF defects were observed with W4.5 and W4.2 stimuli, respectively.

The right eye similarly exhibited signs of cataract formation. The appropriate surgery resulted in a VA of 0.6. Seven months after surgery the subject's vision in her right eye had decreased to 0.1. Only a mild optic disc oedema was observed, which turned to optic atrophy within 2 months (Figure 14). Again, no signs of diabetic retinopathy were found. The VFs displayed a marked constriction of up to 15–20º in the right eye, while only a paracentral remnant of the VF could be detected in the left eye (Figure 16). No VEPs could be recorded.

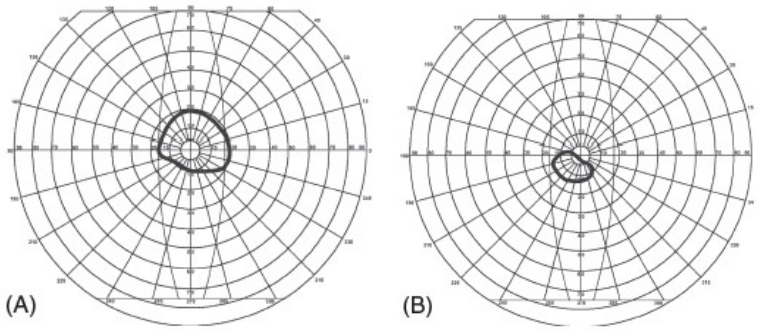

Figure 16. Kinetic VF impairments in the right (A) and left (B) eyes in case 3. There is a marked constriction of the VF in the right eye and a paracentral remnant of the VF in the left eye (W4.5).

Beside NAION no alternative explanation could be found for the subject's sudden visual loss. No neurological signs were present and the cranial and orbital MRI excluded multiplex sclerosis. Chemical blood tests and all immunological tests excluded other pathologies of visual loss.

4.5. Clinical studies V.: Differential diagnosis of concentric visual field defects using electrophysiological methods

128 eyes of 72 patients with concentric VF defect were analyzed in our laboratory between January 1st, 2002 and 31st December, 2005. The patients' clinical and electrophysiological data were analyzed retrospectively. Mean age was 47.6 years with a range of 11–75 years.

The results were compared to control data from 58 healthy, age matched control subjects with no ophthalmological diseases. The clinical characteristics of the patients are listed in Table 10.

Ophthalmological examination included assessments of appropriate VA, refraction and intraocular pressure. Slit-lamp examinations, ophthalmoscopy, and Goldmann perimetry

were carried out as well. Electrophysiological examinations (VEP, PERG and ERG) were recorded according to the standard method described Chapter 3.

The implicit time and the amplitude of the VEP, PERG and ERG waves were analyzed. Data were analyzed with two-way ANOVA. $P < 0.05$ was considered significant.

Among the 72 patients 20 RP, 1 choroidal osteoma, 1 MAR, 2 optic nerve melanocytoma, 11 NAION, 4 dysthyroid ophthalmopathy, 4 toxic neuropathy, 1 diabetic neuropathy, 9 cerebrovascular circulatory disturbances, 5 optic nerve compression caused by intracranial tumors and 7 empty sella syndrome were found. The possibility of malingering had arisen in 3 cases. Although we found electrophysiological alterations in 4 cases, the aetiology remained unclear.

The characteristic electrophysiological alterations of the diseases are listed in Table 11.

Group	**Patients (eyes)**	**Gender**		**Age (year)**		**Degree of visual field defect**		
		Male	Female		Range	>20º	5–20º	<5º
Retinitis pigmentosa	20 (40)	6	14	23,5	12-35	18	13	9
Choroidal osteoma	1 (2)		1	53,0			1	1
MAR	1 (1)		1	43,0				1
Optic disk melanocytoma	2 (2)		2	59,0	58-60		1	
NAION	11 (17)	3	8	61,2	36-75	8	7	2
Dysthyroid ophthalmopathy	4 (8)	1	3	49,7	38-63	4	4	4
Toxic neuropathy	4 (8)	2	2	50,0	47-53		4	4
Diabetic neuropathy	1 (2)		1	49,0		2		
Cerebrovascular disease	9 (18)	2	7	55,8	41-74	5	8	5
Compressive optic neuropathy	5 (10)		5	48,3	40-57	2	4	4
Empty sella syndrome	7 (14)	1	6	44,7	22-72	8	4	2
Functional	3 (6)	1	2	39,5	32-47	2	4	
Unknown aetiology	4 (8)	2	2	35,2	7-72	4	4	

MAR: melanoma associated retinopathy syndrome; NAION: nonarteritic ischaemic optic neuropathy

Table 10. Clinical data of the 72 patients

RP comes first into our mind among the numerous ophthalmological diseases in the case of concentric VF defect. The decrease of retinal function was detected by the extinguished scotopic and maximal ERG. We found residual responses only in four cases, that time the implicit time of the OP was delayed and its amplitude was decreased. Examining the VEPs, we found both normal, and altered answers with pathological wave form, delayed implicit time and decreased amplitude.

The choroidal osteoma of the papillomacular bundle caused choroidal atrophy in the right eye. Both the latencies of the VEP and PERG were markedly delayed, and the amplitude of the VEP was diminished. We did not find any choroidal atrophy in the left eye; however, a concentric VF defect developed in this side, too. The implicit time of the VEP was slightly delayed and the amplitude slightly decreased.

During the 13-years observation period of the melanocytoma in the right eye of our patient the VA decreased, and her VF narrowed. The implicit time and amplitude alterations of the VEP deteriorated, and the implicit time of OP delayed, too.

	PVEP		PERG		Maximal ERG	OP	
	L	A	L	A	A	L	A
Retinitis pigmentosa	■: → → ■: N	↓↓ ↓↓	■: → →	↓↓	↓↓	N	↓↓
Melanoma associated retinopathy syndrome	■: N ■: N	N	■: N	N	negative	N	N
Choroidal osteoma	■: → → ■: → →	↓↓ ↓↓	■: → →	N	N	N	N
Optic disk melanocytoma	■: N ■: N	↓↓ ↓↓	■: N	N	N	→	N
Nonarteritic ischaemic optic neuropathy	■: → → ■: N	↓↓ ↓↓	■: N	↓	N	N	↓
Toxic neuropathy	■: N ■: N	↓ ↓↓	■: N	N	N	N	N
Diabetic neuropathy	■: → → ■: → →	N	■: → →	N	→ →	→	N
Dysthyroid ophthalmopathy	■: N ■: N	N	■: N	N	N	N	N
Compressive optic neuropathy	■: → ■: N	↓ ↓↓	■: N	N	↓	N	↓↓
Cerebrovascular diseases	■: N ■: N	↓ ↓	■: N	↓	N	→→	↓
Empty sella syndrome	■: N ■: N	↓↓ ↓↓	■: N	N	N	N	N
Functional	■: N ■: N	N	■: N	N	N	N	N

(VEP: pattern visual evoked potential, PERG: pattern electroretinogram, ERG: electroretinogram, OP: oscillatory potencial, L: latency, A: amplitude, ↓/→: $p<0,05$, ↓↓ / →→: $p<0,01$)

Table 11. Characteristic electrophysiological alterations in diseases with concentric VF defect.

Decreased VEP amplitude was found in toxic neuropathy.

Our diabetic patient's neuropathy was detected by the VEP, and her maculopathy was diagnosed by the delayed latency of the PERG and the OP.

We did not found any pathological alterations among patients with endocrine orbitopathy.

5. Discussion

General depression or peripheral contraction of the VF can occur in several disorders along the visual pathways; however, psychogenic and technical factors should also be taken into consideration.

Concentric VF defect can be caused by diseases of the retina, the optic nerve, the optic tract and the visual cortex. The pathomechanism of the VF constriction differs in these diseases. The electrophysiological examinations can help the diagnosis in questionable cases. Causes of concentric VF defects are listed in Table 12 (below).

Causes of concentric visual field defects[82]
1. Praeretinal factors
1.1. Pupillary factors
1.2. Media opacities (contact lenses, corneal oedema, scars, cataracts, vitreous haemorrhage)
2. Primary chorioretinal / Photoreceptor dystrophies
2.1. Chorioideremia, Gyrate atrophy
2.2. Myopic degeneration
2.3. Retinitis pigmentosa
2.4. Cancer- and autoimmunity-associated retinopathies (carcinoma associated retinopathy [CAR], melanoma associated retinopathy [MAR])
2.5. Diabetic retinopathy
2.6. Occlusion of central retinal vein
3. Ganglion-cell/ axon- and optic nerve lesions
3.1. Glaucoma
3.2. Ischemic optic neuropathy (NAION)
3.3. Toxic-nutritional-metabolic neuropathy
3.4. Compressive neuropathy
3.5. Severe pre-eclampsia
3.6. Increased intracranial pressure causing optic neuropathy
4. Bilateral occipital infarct (with macular spare of the centrum)
5. Functional visual field loss
5.1. Neurasthenia
5.2. Hysteria
5.3. Malingering
6. Technical factors
6.1. Inappropriate contrast of stimulus-target/background ratio
6.2. Inappropriate correction
6.3. Too rapid target movement
6.4. Slow response times

Table 12. Causes of concentric VF defects

Primary chorioretinal / Photoreceptor dystrophies

Chorioideremia is caused by the XL-R inherited mutations in the chorioideremia gene resulting in a diffuse atrophy of the RPE and the choriocapillaris." The first symptom manifesting in males in early childhood is usually impaired night vision followed by a progressive narrowing of the field of vision (tunnel vision), and later a decrease in the VA. The ophthalmologic features are characteristic; however, the field constriction and the progression of the VA resemble the RP.

The ERG, VEP and mfERG alterations reveal the exact severity of the disease. *Gyrate atrophy* is a rare, AR disorder resulting from the deficiency of the mitochondrial matrix enzyme ornithine-aminotransferase, the gene of which is located on chromosome 10q26. The exact mechanism of chorioretinal degeneration remains unknown.

Clinically, gyrate atrophy patients initially develop myopia and reduced night vision, usually before the end of the first decade of life." Ophthalmoscopy reveals the presence of numerous sharply demarcated circular areas in the peripheral retina which gradually increase in number and size, coalesce, and spread from the peripheral to the central fundus, forming lesions with a "gyrate" or garland-like border. Reduced peripheral vision with constriction of the VFs is obvious in the 2nd decade. Complete loss of vision is associated with involvement of the macula.

ERG abnormalities are already present at an early stage of the disease, with impaired rod and cone responses, progressing to an extinguished response."

In *high myopia* the VF constriction depends on the severity of peripheral degeneration and the ERG turn to be subnormal. However, we can differentiate between this peripheral retinal degeneration and the true degenerative myopia, which is a retinal dystrophy accompanied with myopia. In this case the ERG is extinguished.

The term of *retinitis pigmentosa* (RP) refers to a heterogeneous group of inherited photoreceptor dystrophies characterized by AD, AR and XL-R inheritance patterns, in which the rods and cones undergo progressive degeneration. Over 100 genes can cause RP. The large number of RP genes identified can be grouped into the following functional classes: (1) proteins of the visual cascade, (2) proteins of the visual cycle, (3) photoreceptor cell transcription factors, (4) proteins related to catabolic processes, and (5) genes of unknown function. The 'final common pathway' remains photoreceptor cell death by apoptosis. The outer segments progressively shorten, followed by loss of the rod photoreceptor. This occurs mostly in the mid-periphery of the retina, or, in some cases, the inferior retina, thereby suggesting a role for light exposure.

Affected patients report impaired dark adaptation, night blindness and peripheral vision loss. Although initially there may be only a peripheral ring scotoma, typically from 30° to 50°, with time this scotomatous area breaks out of the periphery and infringes on the central field, until only a small area of vision remains, sometimes associated with a temporal island.

ERG may be severely subnormal or undetectable as soon as in the early stage of the disease. For the follow- up of the progression of the photoreceptor loss, PERG, VEP and mfERG seemed to be appropriate.

The PVEPs are elicited predominantly from the central 10º of the VF, which is well preserved for a long period during the progression of RP. This is why we offer the VEP tests

for evaluation of the progression of the disease. Three types of VEP waveforms were found: normal VEPs, VEPs with bifid pattern and VEPs with broad waveform. These alterations might be reflecting different patterns of the cone receptor loss in the central retina. It may depend on the type of inheritance, the time of the examination, etc. The interpretation of these VEP alterations needs further investigation.

PERGs were severally depressed in all of our patients. Following the photoreceptor loss, transneural degeneration of the ganglion cells can be expected. However, histological examination did not find significant difference in the number of ganglion cells in RP patients with serious or mild visual loss.[7] This result suggests that the visual impairment in RP is determined not only by the extent of degeneration, but also by the localisation of the degenerated patches within the foveal area. This concept is in agreement with our mfERG observations, which revealed involved and intact areas in the central retina.

According to our observations, mfERG can show the involved and intact retinal areas in the central 30º of the VF. The different preserved areas in the two eyes may be complemented in the visual cortex (filling-in phenomenon), which can help visual processing. VEP and PERG alterations in RP are important in the follow-up of the progression.

Further investigations into transneural degeneration are very important for any prospective therapeutic intervention.

In *cancer- and autoimmune-associated retinopathies* autoantibodies directed at various retinal protein antigens cause progressive vision loss. An underlying malignancy places this condition in the category of paraneoplastic syndromes. When no malignancy is found, patients are considered to have autoimmune retinopathy. Recoverin,[7] alfa-enolase and photoreceptor cell-specific nuclear receptor gene product initiate a cascade of events, leading to increased phosphorylation of rhodopsin, which activates apoptotic pathways, resulting in diffuse photoreceptor degeneration with or without inflammation. Ganglion cells and retinal vasculature are spared.

Patients with MAR have IgG autoantibodies that react with human rod bipolar cells antigens.

The clinical features of paraneoplastic retinopathy and autoimmune retinopathy are generally similar. In cases of CAR, vision loss can occur before malignancy is diagnosed.[7,8] In contrast, MAR usually develops years after removal of a malignant melanoma of the skin, often at the stage of skin malignant melanoma metastatic spread.

Symptoms and signs depend on which retinal elements are affected. CAR affects both rods and cones. Patients with CAR usually have prominent involvement of central vision, resulting in markedly decreased VA, loss of colour vision, and central scotomas. Later total blindness develops. In contrast, patients with MAR, when antibodies against bipolar cells

interfere with rod function, often have near-normal VA, colour vision and central VFs. Peripheral or mid-peripheral field loss can usually be demonstrated. Generally, there is no ophthalmologic sign of the disease. Later on, attenuation of the arterioles with thinning and mottling of the RPE may develop.

The ERG alteration (extinguished in CAR syndrome, negative type ERG in MAR syndrome) can draw the attention to the origin of the sometimes unusual symptoms.

Optic neuropathy has been suggested as a specific complication of diabetes, but its nature and pathogenesis are still unclear. Proposed pathophysiological mechanisms include toxic effects of prolonged hyperglycaemia, increased susceptibility of the optic nerves to inflammation in diabetes, a disturbance of schwann cell metabolism, and anterior ischemic optic neuropathy (or vascular pseudopapillitis).[»] Beyond optic neuropathy, peripheral neovascularisation can also result in VF narrowing.

Ganglion-cell, axon- and optic nerve lesions

The diagnosis in *glaucoma is* based on the 'typical' VF defects caused by pressure differences between the intraocular fluid and CSF (rather than the absolute value of the IOP). This difference results in a passive neuronal intracellular fluid flux in the axons of the ganglion cells close to the lamina cribrosa. The location and the thickness of the axons within the optic nerve at the level of the lamina cribrosa determine their sensitivity and susceptibility to damage**.** Intracellular fluid flow locally depletes adenosine triphosphate, disrupting active axonal transport, leading to cell death in turn.

The papillomacular bundle of optic nerve axons, - which, as part of the parvocellular pathway, serve central vision - remain intact for long. PERG is the only objective method for the detection of the ganglion cell damage. During progression more and more axons and ganglion cells will be damaged, resulting in peripheral narrowing of the VF. Glaucoma will cause magnocellular pathway damage.

Nonarteritic anterior ischemic optic neuropathy (NAION) is one of the most frequent causes of sudden visual loss in middle-aged or elderly patients.[»»] Its annual incidence has been estimated to be 10.3 per 100,000 individuals aged 50 years or older. It was be presumed that an infarction of a blood vessel supplying the intrascleral portion of the optic nerve is the cause of the sudden visual loss. The infarction may occur by defective autoregulation, while others have emphasized the importance of an anatomical variation of the optic disk ('disk at risk') as an important predisposing factor.[»] The acute hypoxia of the optic nerve head results in axoplasmic flow stasis in the optic nerve fibers, swallowing the axons in the level of the cribriform plate of the disk. The fall of perfusion pressure in the optic disc capillaries due to nocturnal arterial hypotension and elevation of IOP results in marked ischemia and that precipitates visual loss, which is usually discovered when waking up in the morning.

The type and severity of the axon loss can be evaluated by VF examination, provided that the visual acuity is good enough for fixation. In the acute stage it can be an arcuate defect, but later all the four quadrants of the VF can be constricted resulting in an indefinite concentric defect.

Electrophysiological examination shows the severity of the axon damage and in young patients – when the manifestation of this disease is rare –, thus helping differential diagnosis.

Arteritic ischemic optic neuropathy (AION) is a sight-threatening autoimmune disease caused by giant cell vasculitis of the medium arteries. We stress the importance of differentiation between AION and NAION because of their different treatment and prognosis. Blindness can occur by central retinal artery occlusion or ischaemic optic neuropathy.

Toxic-nutrition-metabolic neuropathy can be caused by exogenous or endogenous factors. If the subchiasmatic part of the optic nerve is the site of the damage, bilateral central scotomas or a narrowing of the peripheral visual field will develop. VEPs are subnormal in these cases, while ERGs are normal.

There are drugs (thioridasine and indometacinum) which cause RPE lesion followed by depigmentation and atrophy of the retina. ERGs are subnormal or extinguished in such cases.

Vigabatrin can cause retinal cone dysfunction. An idiosyncratic drug reaction within the neurosensory retina may underlie the pathogenesis of the VF loss with interindividual susceptibility. Vigabatrin causes irreversible inhibition of GABA aminotransferase with consequent elevation of GABA.[7] Sildenafil (Viagra), vardenafil and tadalafil are selective inhibitors of cyclic guanosine monophosphate specific phosphodiesterase 5. Phosphodiesterase 6 isoenzyme is found predominantly in retinal photoreceptors and is very important in the phototransduction cascade.

Tobacco, alcohol, chloramphenicol and ethambutol cause ganglion cell loss. The pathogenesis of tobacco–alcohol amblyopia remains elusive; combined mechanisms of toxic insults from tobacco compounds and/or ethyl alcohol might be at play, concurrent with nutritional deficiencies.[7] Tobacco-derived compounds including reactive oxygen species and cyanide reduce mitochondrial respiratory activity, damage mitochondrial DNA, and induce alterations of mitochondrial morphology.

Chloramphenicol is well known to inhibit mitochondrial protein synthesis, causing retinal ganglion cell and nerve fiber loss, with demyelinisation of the optic nerve, involving predominantly the papillomacular bundle.

Ethambutol might interact with Cu-containing cytochrome oxydase c (complex IV) and Fe-containing NADH:Q oxidoreductase (complex I), thus damaging the mitochondrial respiratory chain, inducing axonal swelling in the optic chiasm and in the intracranial portion of the optic nerve.

Tetracycline, minocycline, lithium, Accutane, nalidixic acid, and corticosteroids (both use and withdrawal) can cause benign intracranial hypertension and papilledema.

In *compressive optic neuropathy*, beside the direct compression that the tumor exerts on the optic nerve, a general intracranial pressure elevation has to be taken into account. Peripheral axons will suffer the direct effect of compression and disturbances of the axoplasmic and blood flow.

Infiltrative neuropathy - sarcoidosis, tuberculosis, cryptococcus infection, leukaemia, lymphoma, and metastatic cancer) can also result in VF narrowing.

The disc swelling in *papilloedema* is the result of axoplasmic flow stasis with intra-axonal oedema in the area of the optic disc. The subarachnoid space of the brain is continuous with the optic nerve sheath. Thus, as the CSF pressure increases, the pressure is transmitted to the optic nerve, and the optic nerve sheath acts as a tourniquet to impede axoplasmic transport. This leads to a buildup of material at the level of the lamina cribrosa, resulting in the characteristic swelling of the nerve head.

Bilateral occipital infarct (with macular spare of the centrum)

The posterior cerebral artery supplies the visual cortex. There are many causes of the *bilateral posterior cerebral artery occlusion*: multiple emboli from a mural thrombus of the vertebral or basilar artery, etc. The visual cortex has a secondary blood supply from the carotid system. In infarction of both occipital lobes, the accessory blood supply from the carotid system may preserve the macular projection. A person with bilateral occipital infarct with macular sparing will present with a preserved central acuity but only a small field, usually 2 to 3°, which means functional blindness.

Functional field defects

Patients with *functional VF loss* can be placed into one of three general groups: neurasthenics, hysterics, or malingerers. The neurasthenic patient usually has many complaints, not limited to the visual system, or to the field loss. The degree of field or visual defect varies from one examination to another, sometimes during the examination as well. The patient with hysteria has a single ocular complaint. The malingerer may be the most difficult patient with functional loss, particularly if he has previously been examined by another physician, and has acquired more experience with field testing than he had when first examined.

Severely contracted VFs can also be seen in exacting patients who want to be sure they see the object and, therefore, unduly contract the fields.

The PVEP is useful to determine the organic origin of the visual loss.

6. Summary

Several diseases causing lesions along the visual pathways can result in concentric VF defect. In the discussion we collected these diseases and analysed the possible pathological processes that may result in VF defects. The aim of our investigation was to find the appropriate electrophysiological method or combination of methods for objective evaluation of the functional loss in these disorders.

For this purpose the first step was to introduce the modern, standard electrophysiological methods into the clinical practice in Hungary.

1. We determined the normal parameters of standard ERG, mfERG, PERG and PVEP and published our first experiences.
2. We drew attention to the importance of combined use of electrophysiological methods, especially in the neuroophthalmological practice.
3. We observed three types of mfERG alterations in RP. Further we found better preserved focal areas within the central visual field. The mfERG results were against the continuous degeneration of the photoreceptors towards the fovea. These where better preserved areas in the central retina, which may help the analysis of the visual information in the visual cortex in patients with RP.
4. Although ERG examinations have priority in the diagnosis of RP, we point to the importance of PERG and PVEP tests in the determination of the progression of the disease. The three types of VEP alterations may reflect not only the severity of the functional loss in the foveal area but may indicate histological different photoreceptor damage, too.
5. We were the first to publish a monocular case of MAR syndrome.
6. Our investigation in NAION patients was important not only in the evaluation of the severity of visual deficits, but also provided further help to solve differential diagnostic problems in young patients with acute visual loss with papilloedema.

7. Conclusions

The electrophysiological investigations are not widely used in the ophthalmological practice, although they are the methods to objective evaluation of the functional loss along the visual pathway.

Different disorders resulted in concentric VF loss. The combined use of this methods help to find the origin of the field loss, help to differential diagnosis in the cases when clinical symptoms, the visual loss and the ophthalmoscopic alterations are not in agreement.

This new methods may give new information on the pathophysiology of the disorders of visual pathway.

8. Acknowledgements

I am indebted to Prof. Dr. Márta Janáky, Prof. Dr. György Benedek and Prof. Dr. Lajos Kolozsvári who provided me a chance to participate in this research.
I also thank Kati Mayer and Gabriella Dósai-Molnár for their valuable technical assistance.

9. References

1. Andres DA, Seabra MC, Brown MS, Armstrong SA, Smeland TE, Cremers FP, Goldstein JL: cDNA cloning of component A of Rab geranylgeranyl transferase and demonstration of its role as a Rab escort protein. Cell 1993; 73: 1091-9.
2. Ballinger SW, Bouder TG, Davis GS, Judice SA, Nicklas JA, Albertini RJ: Mitochondrial genome damage associated with cigarette smoking. Cancer Res 1996; 56: 5692-7.
3. Beck RW, Servais GE, Hayreh SS: Anterior ischemic optic neuropathy. IX. Cup-to-disc ratio and its role in pathogenesis. Ophthalmology 1987; 94: 1503–8.
4. Bernal S, Calaf M, Garcia-Hoyos M, Garcia-Sandoval B, Rosell J, Adan A, Ayuso C, Baiget M: Study of the involvement of the RGR, CRPB1, and CRB1 genes in the pathogenesis of autosomal recessive retinitis pigmentosa. J Med Genet 2003; 40: e89.
5. Berson EL, Lessel S: Paraneoplastic night blindness with malignant melanoma. Am J Ophthalmol 1988; 106: 307-11.
6. Bodis-Wollner I, Ghialardi MF, Mylin LH: The importance of stimulus selection in VEP practice: the clinical relevance of visual physiology. In: Cracco R.Q., Bodis-Wollner I., eds. Frontiers of Clinical Neuroscience: Evoked Potentials. New York: A.R Liss; 1986: 17-27.
7. Boone MI, Massry GG, Frankel RA, Holds JB, Chung SM: Visual outcome in bilateral nonarteritic anterior ischemic optic neuropathy. Ophthalmology 1996; 103: 1223–28.
8. Borchert M, Lessell S: Progressive and recurrent nonarteritic anterior ischemic optic neuropathy. Am J Ophthalmol 1988; 106: 443–49.
9. Brian L, Norris FH: The Remote Effects of Cancer on the Nervous System. New York, Grune and Stratton, 1965; 24.
10. Burde RM: Optic disk risk factors for nonarteritic anterior ischemic optic neuropathy. Am J Ophthalmol 1993; 116: 759–64.
11. Bush RA, Sieving PA: A proximal retinal component in the primate photopic ERG a-wave. Invest Ophthalmol Vis Sci 1994; 35: 635-45.
12. Caton R: The electrical currents of the brain. BJO 1875; 2: 278.

13. Daniel PM, Whitteridge D: The representation of the visual field on the cerebral cortex in monkeys. J Physiol. 1961; 59: 203-21.
14. Follmann P: Kinetikus perimetria: alapelv, gyakorlat, értékelés, hibalehetőségek. In: Follmann P (ed) A látótér vizsgálata. Tömő utcai füzetek Semmelweis Egyetem, I. sz. Szemészeti Klinika, Budapest, 2000.
15. François J: Vascular pseudopapillitis: ischemic optic neuropathy. Ann Ophthalmol 1976; 8: 901-19.
16. François J: Gyrate atrophy of the choroid and retina. J. Ophthalmologica. 1979; 178: 311-320.
17. Gilman AG: 1985. Goodman and Gilman's the Pharmacological Basis of Therapeutics, 7th Edition. Macmillan, New York, pp. 1179–1183.
18. Giordano L, Valseriati D, Vignoli A, Morescalchi F, Gandolfo E: Another case of reversibility of visual field defects induced by vigabatrin monotherapy: is young age a favourable factor? Neurol Sci 2000; 21: 185−186.
19. Green DG, Kapousta-Bruneau NV: A dissection of the electroretinogram from the isolated rat retina with microelectrodes and drugs. Vis Neurosci 1999; 16: 727-41.
20. Grover S, Fishman GA, Brown J: Patterns of visual field progression in patients with retinitis pigmentosa. Ophthalmology 1998; 105: 1069-1075.
21. Gurevich L, Slaughter MM: Comparison of the waveforms of the ON bipolar neuron and the b-wave of the electroretinogram. Vision Res 1993; 33: 2431-5.
22. Guyer DR, Miller NR, Auer CL, Fine SL: The risk of cerebrovascular and cardiovascular disease in patients with anterior ischemic optic neuropathy. Arch Ophthalmol 1985; 103: 1136–42.
23. Harley RD, Huang NN, Macri CH, Green WR: Optic neuritis and optic atrophy following chloramphenicol in cystic fibrosis patients. Tr. Am. Acad. Ophth. Otol. 1970; 74: 1011–31.
24. Harrison JM, O'Connor PS, Young RS, Kincaid M, Bentley R: The pattern ERG in man following surgical resection of the optic nerve. Invest Ophthalmol Vis Sci 1987; 28: 492–99.
25. Hattenhauer MG., Leavitt JA., Hodge DO., Grill R, Gray DT: Incidence of nonarteritic anterior ischemic optic neuropathy. Am J Ophthalmol 1997; 123: 103–7.
26. Hayreh SS, Joos KM, Podhajsky PA, Long CR: Systemic diseases associated with nonarteritic anterior ischemic optic neuropathy. Am J Ophthalmol 1994; 118: 766–80.
27. Hayreh SS, Podhajsky PA, Zimmerman B: 1997b. Nonarteritic anterior ischemic optic neuropathy: time of onset of visual loss. Am. J. Ophthalmol 1997; 124: 641–47.

28. Holder GE: Pattern electroretinography (PERG) and an integrated approach to visual pathway diagnosis. Progr Retin Eye Res 2001; 20: 531-561.
29. Hood DC, Bach M, Brigell M, Keating D, Kondo M, Lyons JS, Palmowski-Wolfe AM: ISCEV Guidelines for clinical multifocal electroretinography (2007 edition). Doc Ophthalmol 2008; 116: 1-11.
30. Hood DC, Birch DG: Assessing abnormal rod photoreceptor activity with the a-wave of the electroretinogram: applications and methods. Doc Ophthalmol 1997; 92: 253-67.
31. Hood DC., Birch DG: Beta wave of the scotopic (rod) electroretinogram as a measure of the activity of human on-bipolar cells. J opt Soc Am Opt Image Sci Vis 1996; 13: 623–33.
32. Hood DC, Birch DG: The A-wave of the human electroretinogram and rod receptor function. Invest Ophthalmol Vis Sci 1990; 31: 2070-81.
33. Kaiser-Kupfer MI., Ludwig F, DeMonasterio: Gyrate atrophy of the choroid and retina. Early findings. Ophthalmology. 1985; 92: 394-401.
34. Karwoski CJ, Xu X: Current source-density analysis of light evoked field potentials in rabbit retina. Vis Neurosci 1999; 16: 369-77.
35. Keltner JL, Roth AM, Chang RS: Photoreceptor degeneration: Possible autoimmune disorder. Arch Ophthalmol 1983; 101: 564-69.
36. Keltner JL, Thirkill CE, Yip PT: Clinical and immunologic characteristics of melanoma-associated retinopathy syndrome: eleven new cases and a review of 51 previously published cases. J Neuroophthalmol 2001; 21: 173–87.
37. Kennedy JR, Elliot AM: Cigarette smoke: the effect of residue on mitochondrial structure. Science 1970; 168, 1097–98.
38. Kornguth SE, Klein R, Appen R: Occurrence of anti-retinal ganglion cell antibodies in patients with small cell carcinoma of the lung. Cancer 1982; 50: 1289-93.
39. Kozak SF, Inderlied CB, Hsu HY, Heller KB, Sadun AA: The role of copper on ethambutol's antimicrobial action and implications for ethambutol-induced optic neuropathy. Diagn Microbiol Infect Dis 1998; 30: 83-7.
40. Kraemer G, Ried S, Landau K, Harding GFA: Vigabatrin. Reversibility of severe concentric visual field defects after early detection and drug withdrawal: a case report. Epilepsia 2000; 41 Suppl: 144.
41. Lamb TD, Pugh EN: A quantitative account of the activation steps involved in phototransduction in amphibian photoreceptors. J Physiol 1992; 449: 719-58.
42. Lessell S: Nonarteritic anterior ischemic optic neuropathy: enigma variations. Arch Ophthalmol 1999; 117: 386–88.

43. Mansour AM, Shoch D, Logani S: Optic disk size in ischemic optic neuropathy. Am J Ophthalmol 1988; 106: 587–89.
44. Marmor MF, Holder GE, Seliger MW, Yamamoto S: Standard for clinical electroretinography (2004 update) Doc Ophthalmol 2004; 108: 107–114.
45. Marmor MF., Fulton AB, Holder GE, Miyake Y, Brigell M, Bach M: ISCEV Standard for full-field clinical electroretinography (2008 update). Doc Ophthalmol 2009; 118: 69-77.
46. Mayreh SS: Anterior ischaemic neuropathy. New York. Springer-Verlag, 1975; p. 122.
47. Miller GR, Smith JL: Ischemic optic neuropathy. Am J Ophthalmol 1966; 62: 103-15.
48. Newman EA, Odette LL: Model of electroretinogram b-wave generation: a test of the K$_t$ hypothesis. J Neurophysiol 1984; 51: 164-82.
49. Newman WD, Tocher K, Acheson J: Vigabatrin associated visual field loss: a clinical audit to study prevalence, drug history and effects of drug withdrawal. Eye 2002; 16: 567−71.
50. **Pálffy A**, Janáky M, Fejes I, Horváth G, Benedek G: Interocular amplitude differences of multifocal electroretinograms obtained under monocular and binocular stimulation conditions. Acta Physiologica (Accepted to publication)
51. Polans AS, Burton MD, Haley TL, Crabb JW, Palczewski K: Recoverin, but not visinin, is an autoantigen in the human retina identified with a cancer-associated retinopathy. Invest Ophthalmol Vis Sci 1993; 34: 81-90.
52. Pryor WA, Arbour NC, Upham B, Church DF: The inhibitory effect of extracts of cigarette tar on electron transport of mitochondria and submitochondrial particles. Free Radic Biol Med 1992; 12: 365–72.
53. Raitta C, Carlson S, Vannas-Sulonen K: Gyrate atrophy of the choroid and retina: ERG of the neural retina and the pigment epithelium. Br J Ophthalmol. 1990; 74: 363-67.
54. Repka MX, Savino PJ, Schatz NJ, Sergott RC: Clinical profile and longterm implications of anterior ischemic optic neuropathy. Am J Ophthalmol 1983; 96: 478–83.
55. Rizzo JF, Lessell S: Tobacco amblyopia. Am J Ophthalmol. 1993; 116: 84-7.
56. Robson JG, Frishman LJ: Dissecting the dark-adapted electroretinogram. Doc Ophthalmol 1998; 95: 187-215.
57. Robson JG., Frishman LJ: Response linearity and kinetics of the cat retina: the bipolar cell component of the dark-adapted electroretinogram. Vis Neurosci 1995; 12: 837-50.
58. Rovamo J, Virsu V: An estimation and application of the human cortical magnification factor. Exp Brain Res. 1979; 37: 495-510.

59. Santos A, Humayun MS, de Juan E Jr, Greenburg RJ, Marsh MJ, Klock IB, Milam AH: Preservation of the inner retina in retinitis pigmentosa. A morphometric analysis. Arch Ophthalmol 1997; 115: 511–15.
60. Sawyer RA, Selhorst JB, Zimmerman LE: Blindness caused by photoreceptor degeneration as a remote effect of cancer. Am J Ophthalmol 1976; 81: 606-13.
61. Seabra MC, Brown MS, Goldstein JL: Retinal degeneration in choroideremia: deficiency of rab geranylgeranyl transferase. Science 1993; 259: 377-81.
62. Seabra MC, Brown MS, Slaughter CA, Südhof TC, Goldstein JL: Purification of component A of Rab geranylgeranyl transferase: possible identity with the choroideremia gene product. Cell 1992; 70: 1049-57.
63. Shiells RA, Falk G: Contribution of rod, on-bipolar and horizontal cell light responses to the ERG of dogfish retina. Neuroscience 1999; 16: 503-11.
64. Shiraki H: Neuropathy due to intoxication with anti-tuberculous drugs from neuropathological viewpoint. Adv Neurol Sci 1973; 17: 120.
65. Skillern PG, Lockhart G: Optic neuritis and uncontrolled diabetes mellitus in 14 patients. Ann Intern Med. 1959; 51: 468-75.
66. Solberg Y, Rosner M, Belkin M: The association between cigarette smoking and ocular diseases. Surv Ophthalmol. 1998; 42: 535-47.
67. Stockton RA, Slaughter MM: B-wave of the electroretinogram. A reflection of ON bipolar cell activity. J Gen Physiol 1989; 93: 101-22.
68. Stone JL, Barlow WE, Humayun MS, de Juan E Jr, Milam AH: Morphometric analysis of macular photoreceptors and ganglion cells in retinas with retinitis pigmentosa. Arch Ophthalmol 1997; 110: 1634–39.
69. Sutter EE, Tran D: The field topography of ERG components in man. I. The photopic luminance response. Vision Res 1992; 32: 433–46.
70. Sutter EE: The fast m-transform: a fast computation of cross-correlations with binary m-sequences. Soc Ind Appl Math 1991; 20: 686-94.
71. Takki K, Simell O: Genetic aspects in gyrate atrophy of the choroid and retina with hyperornithinemia. Br J Ophthalmol. 1974; 58: 907-16.
72. Takki K, Milton R: The natural history of gyrate atrophy of the choroid and retina. Ophthalmology. 1981; 88: 292-301.
73. Thirkill CE, Tait RC, Tyler NK, Roth AM, Keltner JL: Antibodies in patients with CAR are directed toward recoverin. The cancer-associated retinopathy antigen is a recoverin-like protein. Invest Ophthalmol Vis Sci 1992; 33: 2768-72.

74. Thomas PK, Lascelles RG: Schwann-cell abnormalities in diabetic neuropathy. Lancet. 1965; 1: 1355-7.
75. Tian N, Slaughter MM: Correlation of dynamic responses in the ON bipolar neuron and the b-wave of the electroretinogram. Vision Res 1995; 35: 1359-64.
76. Varga G., Fejes I, Papp F, Janáky M.: Atypical gyrate atrophy – a case report. Szemészet 2009; 146; 147-153.
77. Vaugham HG, Katzman R: Evoked responses in visual disorders. Ann N.Y. Acad Sci 1964; 112: 305-19.
78. Viswanathan S, Frishman LJ, Robson JG: The uniform field and pattern ERG in macaques with experimental glaucoma: removal of spiking activity. Invest Ophthalmol Vis Sci 2000; 41: 2797–810.
79. Wachtmeister L: Oscillatory potentials in the retina: what do they reveal? Prog Retin Eye Res 1998; 17: 485-521.
80. Waite JH, Beetham WP : The visual mechanism in diabetes mellitus. New England J Med 1935; 212: 367: 429.
81. Weleber RG, Watzke RC, Shults WT, Trzupek KM, Heckenlively JR, Egan RA, Adamus G: Clinical and electrophysiologic characterization of paraneoplastic and autoimmune retinopathies associated with antienolase antibodies. Am J Ophthalmol 2005; 139: 780–94.
82. Wirtschafter JD: Anatomic Basis and differential diagnosis of field defects. In: Walsh T.J. (ed.): Visual Fields: Examination and interpretation. 2nd ed. American Academy of Ophthalmology, San Francisco 1990; 45-46.
83. Xu X, Karwoski CJ: Current source density analysis of retinal field potentials. II. Pharmacological analysis of the b-wave and M-wave. J Neurophysiol 1994; 72: 96-105.